SYNTHESIS AND CHARACTERIZATION OF CRYSTALLINE COMPLEXES OF DIMETHYL SULFOXIDE WITH HOLMIUM AND PRASEODYMIUM BROMIDES

By

CHARLES LEE RIGGS II

Bachelor of Science

Southwestern State College

Weatherford, Oklahoma

1967

Submitted to the Faculty of the Graduate College
of the Oklahoma State University
in partial fulfillment of the requirements
for the Degree of
DOCTOR OF PHILOSOPHY
May, 1974

SYNTHESIS AND CHARACTERIZATION OF CRYSTALLINE COMPLEXES OF DIMETHYL SULFOXIDE WITH HOLMIUM AND PRASEODYMIUM BROMIDES

Thesis Approved:

I. Dwaine Eubanks
Thesis Adviser

Tom E. Moore

Robert Thurman

Lester W. Reed

N. D. Durham
Dean of the Graduate College

ACKNOWLEDGEMENTS

The author would like to especially express gratitude to Dr. I. Dwaine Eubanks for his patience and guidance throughout this study. Appreciation is expressed to Dr. J. Paul Devlin and Gary Ritzhaupt for their assistance in obtaining the Raman spectra and to Dr. Robert D. Freeman for the use of the x-ray facilities and for serving on the committee.

Gratitude is also expressed to Dr. Lester W. Reed and Dr. Tom E. Moore for serving on the committee.

Special thanks is extended to Dr. Dick van der Helm of the University of Oklahoma for teaching the author the elements of x-ray crystalography.

TABLE OF CONTENTS

LIST OF TABLES

LIST OF FIGURES

LIST OF FIGURES (Continued)

GLOSSARY OF SELECTED SYMBOLS AND ABBREVIATIONS

acac	Acetylacetonate
BuL	γ-Butyrolactam
CMP	Diisopropyl-N,N-diethylcarbamylmethylenehonate
CN	Coordination number
DMF	Dimethyl formamide
DMSO	Dimethyl sulfoxide
dpm	Dipivalomethanate
DPSO	Diphenyl sulfoxide
EDAN	N,N'-Ethylenedianthranilic acid
EDDA	N,N'-Ethylenediamine-diacetic acid
EDTA	Ethylenediaminetetraacetic acid
en	Ethylenediamine
G	Density
HCPC	1-Hydroxycylopentanecarboxylic acid
n	Integer
n_1	Number of DMSO molecules per unit of $PrBr_3$
n_2	Number of DMSO molecules per unit of $HoBr_3$
pn	1,2-Propanediamine
py	Pyridine
R	Camera radius in mm
TMSO	Tetramethylene sulfoxide
TMU	Tetramethylurea
Z	Number of molecules per unit cell

CHAPTER I

INTRODUCTION

Historical

The lanthanide elements, of which holmium and praseodymium are representative, are strictly the fourteen elements following lanthanum in which the fourteen 4f electrons are being successively added to the lanthanum configuration. Since the term lanthanide is used to indicate that these elements form a closely allied group, for the chemistry of which lanthanum is the prototype, the series is often taken as including lanthanum itself and will be so used in this paper (1,2,3).

The lanthanide elements were originally known as the rare earth elements from their occurrence in oxide mixtures (1). They are not, however, particularly rare elements. Elements such as cerium, lanthanum, and neodymium are as abundant as lead and tin, and even the least abundant of the naturally occurring rare earths are far more plentiful than the platinum-group metals.

Extensive literature dealing with the lanthanides dates back to approximately 1800 (2). However, early researchers in the area were severely hampered by the difficulty of separating any one lanthanide from the others due to their close proximity in chemical properties. Now, largely as a by-product of technology developed by U.S. Atomic Energy Commission activities, quantities of these materials of high purity are readily available.

The chemistry of the lanthanides is predominately that of the tripositive cations. For several of the lanthanides, other oxidation states occur although these are always less stable than the characteristic tripositive state (1,2,3). Table I lists the observed oxidation states, electronic configurations, and crystal radii of the lanthanides. As indicated by Table I, the tripositive oxidation state is by far the most prevalent. Another interesting feature of Table I is the change in the crystal radii with increasing atomic number. In the lanthanide series, addition of electrons to the 4f orbitals cannot counterbalance the increase in nuclear charge that occurs; size therefore decreases. This decrease is the well-known "lanthanide contraction" (1,2). Among the tripositive species, crystal radii decrease smoothly from La^{3+} to Gd^{3+} and then smoothly from Gd^{3+} to Lu^{3+}, but a slight break at Gd^{3+} does occur (1,2). Correspondingly, many other properties of the trivalent lanthanides are observed to show a break at Gd^{3+} (1). The lanthanide contraction is responsible for the small variation in properties that permits separation of the lanthanides by fractionation methods. The lanthanide contraction may be related also to the increasing reduction potential of the metal ions with increasing atomic number (1,3,4).

In most respects, the chemistry of the trivalent lanthanides is similar to that of the alkaline earth metals (1,3). They form oxides, Ln_2O_3, which resemble the Ca, Sr, Ba group oxides and absorb carbon dioxide and water from the air to form carbonates and hydroxides, respectively (1).

Some similarities between the lanthanides and the d-type transition elements might be expected, particularly in the formation of complex species. In the d-type transition metals, complex formation is primarily

TABLE I

OBSERVED OXIDATION STATES OF THE LANTHANIDES

Element	Outer Electronic Configuration (13)				Crystal Radius (14)			
	M	M^{2+}	M^{3+}	M^{4+}	M	M^{2+}	M^{3+}	M^{4+}
La	$5d^16s^2$		Xe		1.885		1.061	
Ce	$4f^26s^2$		$4f^1$	Xe	1.825		1.034	0.92
Pr	$4f^36s^2$		$4f^2$	$4f^1$	1.836		1.013	0.90
Nd	$4f^46s^2$	$4f^4$	$4f^3$	$4f^2$	1.829		0.995	
Pm	$4f^56s^2$		$4f^4$				0.979	
Sm	$4f^66s^2$	$4f^6$	$4f^5$		1.811	1.11	0.964	
Eu	$4f^76s^2$	$4f^7$	$4f^6$		1.944	1.09	0.950	
Gd	$4f^75d^16s$		$4f^7$		1.810		0.938	
Tb	$4f^96s^2$		$4f^8$	$4f^7$	1.801		0.923	0.84
Dy	$4f^{10}6s^2$		$4f^9$	$4f^8$	1.795		0.908	
Ho	$4f^{11}6s^2$		$4f^{10}$		1.789		0.894	
Er	$4f^{12}6s^2$		$4f^{11}$		1.779		0.881	
Tm	$4f^{13}6s^2$	$4f^{13}$	$4f^{12}$		1.769	0.94	0.869	
Yb	$4f^{14}6s^2$	$4f^{14}$	$4f^{13}$		1.940	0.93	0.858	
Lu	$4f^{14}5d^16s^2$		$4f^{14}$		1.752		0.848	

due to interaction between the d electrons of the valence shell and the ligands (5,6,7,8,9,10,11,12). By analogy to the d-transition metals, the lanthanides might be expected to form complexes by interaction of the f electrons with the ligands. Indeed, it is true that the lanthanides form complexes, and numerous papers have been written postulating the effect of the f electrons in bonding (15,16,17,18,19).

Geschneider (15) has proposed two types of f-electrons, "atomic" 4f electrons and 4f "band" electrons. The band electrons are proposed to be important in forming metal-metal bonds and in explaining the observed melting points, heats of sublimation, and crystal structure of the lanthanide metals. However, no attempt has been made to extend his proposed model to coordination compounds.

Volkov and co-workers (19) proposed that for higher coordination polyhedra of the lanthanides, 34.8 to 46.2% contribution from the f orbitals was necessary to form the polyhedra. However, this view is not commonly accepted and most researchers assume only very small participation by the f orbitals.

Katzin and Barnett (18) have reported spectral evidence for covalent bonding in the lanthanides involving hybridization of the f orbitals. The spectral changes are, however, very small when compared to the spectral changes observed in the d transition series.

Most researchers in the area of lanthanide coordination compounds propose that the formation of coordination compounds of the lanthanides is due primarily to an electrostatic interaction between the trivalent lanthanides and the coordinated ligands (3,20,21,22,23,24,25,26). The general conclusion is that the f electrons of the lanthanides are too well shielded to interact in the same manner as the d electrons of the

d-type transition metals. Each trivalent lanthanide is effectively an inert ion, like those of the alkaline earth metals, that attracts ligands only by overall electrostatic forces. This implies that the more electonegative ligands will be the strongest coordinating ligands.

Numerous coordination compounds of the lanthanides have been reported as summarized in Table II. Most of the compounds are derived from oxygen donor ligands and a few from nitrogen and sulfur donor ligands. Moeller, Dieck, and McDonald (27) have found the same basic trends in coordination number for nitrogen and sulfur donors as for oxygen donor ligands.

The abbreviations used in Table II are listed in the glossary of this thesis. Unless indicated otherwise, the coordination number is for the solid. As indicated in Table II, the lanthanides form complexes with a large variety of ligands and anions. The ligands vary from monodentate, such as water and dimethyl sulfoxide, to hexadentate ligands such as ethylenediaminetetraacetic acid. Coordination numbers for the lanthanide ions vary from six to eleven. Many researchers (28,29,30,31, 32,33,34,35) propose that the coordination number of the lanthanides changes, usually decreasing, at or near gadolinium.

Muetterties and Wright (36) have described the probable geometries for polyhedra of coordination numbers five, six, seven, eight, nine, ten, eleven, twelve, fourteen, and twenty. A basic trend is noted that describes most of the coordination polyhedra. Beginning with a basic geometry of either a trigonal prism or an octahedron, coordination polyhedra for higher coordination numbers can be achieved by capping the basic polyhedra with one, two, or three ligands. For coordination number eight, two of the most frequently reported polyhedra are the dodecahedron

TABLE II

COORDINATION NUMBER OF COMPLEXES OF THE TRIVALENT LANTHANIDE ELEMENTS

Anion/Ligand	Ref.	La	Ce	Pr	Nd	Sm	Eu	Gd	Tb	Dy	Ho	Er	Tm	Yb	Lu	Remarks
ClO_4^-/HCPC	41	9	9	9	9	9	9	9	9	9	9	9	9	9	9	CN in solution. Ligand changes from tridentate to bidentate.
ClO_2^-/H_2O	42	9														CN based on x-ray structure.
EDTA/H_2O	43	10														CN based on x-ray structure.
NO_3^-/bipyridyl	44	10														CN based on x-ray structure.
ClO_4^-/DMSO	35	9			9			9			8				7	CN in solution. Based on calorimetric studies.
ClO_4^-/DMSO	30	8	8	8	8	8	8	8	8	7	7	7	7	7	7	CN based on analysis and spectra.
ClO_4^-/DMSO	45	8	8	8	8	7	7									CN based on conductance and cryoscopic studies.
NO_3^-/DMSO	46 25	10														CN based on x-ray structure. All NO_3^- were found to be bidentate.
ClO_4^-/TMSO	29	8	8	8	8	8	8	8	7½	7½	7½	7½	7	7	7	CN based on analysis, conductance, and spectra.
ClO_4^-/TMU	47	6	6	6	6	6	6	6	6	6	6	6	6	6	6	CN based on analysis, conductance, and spectra.

TABLE II (Continued)

Anion/Ligand	Ref.	La	Ce	Pr	Nd	Sm	Eu	Gd	Tb	Dy	Ho	Er	Tm	Yb	Lu	Remarks
Cl^-/H_2O iminodiacetate	48				9											CN based on x-ray structure.
NO_3^-/BuL	28	8			8			8		7		7		7		CN based on analysis, conductance, and spectra.
NO_3^-/en	32	9		9	9	9	8	8	8	8	8	8		8		Number of coordinated en is constant, number of coordinated anions decrease.
Cl^-/en	32	9			9	8		8				8				
Br^-/en	32	8		8	8											
piperidinium/ benzoylacetonate	49						8									CN in solution.
Diphenyl-propanedionate/ H_2O	50										7					CN based on x-ray structure.
NO_3^-/DMSO	34	8	8	8	8	8		8			7			7		CN based on analysis, conductance, and spectra.
ClO_4^-/DMSO	33	8	8	8	8	7	7	7	7	7	7	6	6	6	6	CN based on analysis and spectra.
acac	51													7		CN based on x-ray structure.
Cl^-/DMSO	52 60	8	8	8	8	8		8								Cl^- in inner coordination sphere. One Cl^- believed to form a bridge.

TABLE II (Continued)

Anion/Ligand	Ref.	La	Ce	Pr	Nd	Sm	Eu	Gd	Tb	Dy	Ho	Er	Tm	Yb	Lu	Remarks
dpm/py	53						8									CN based on x-ray structure.
dpm/4-picoline	37										8					CN based on x-ray structure.
dpm/H_2O	54									7						CN based on x-ray structure.
NO_3^-/EDDA	55	6+		6+	6+	6+	6+	6+	6+	6+	6+	6+	6+	6+	6+	CN in solution.
NO_3^-/DMSO	56	7+	7+	7+	7+	7+		7+								CN depends on how many of the NO_3^- are bidentate.
ClO_4^-/DPSO	57	6	6	6	6	6		6			6			6		CN based on conductance and cryoscopic studies.
acac	58							8	8	8	8	8				Complexes are believed to be dimeric.
ClO_4^-/DMF	59	8	8	8	8	8										CN based on conductance and spectra.
tartrate/H_2O	61						8		8							CN in solution.
dpm/3,3-dimethyl-thietane 1-oxide	62						7									CN based on x-ray structure.
dpm/py	63						8									CN based on x-ray structure.
NO_3^-/CMP H_2O	64	CN varies from a maximum of 10 or 11 to a minimum of 7 or 8														Variation due to possible addition of H_2O to coordination sphere and/or changing the coordination of one or more of the NO_3

TABLE II (Continued)

Anion/Ligand	Ref.	La	Ce	Pr	Nd	Sm	Eu	Gd	Tb	Dy	Ho	Er	Tm	Yb	Lu	Remarks
EDAN/H_2O	31	7	8	8	8	8	7	8	7	7	7	8	7			CN based on x-ray debyegrams and infrared data assuming a dimer type structure.

and the square antiprism. The two are very similar in structure, varying only in the amount of bend present in the square faces of the antiprism structure (23). Many researchers have reported the polyhedra for eight coordination as being either a distorted square antiprism or a distorted D_{2d} dodecahedron (25,37,38,39,40). Since the two structures are so similar and the reported polyhedra are intermediate between the two structures, the choice of nomenclature is only a matter of taste for the author.

In summarizing the chemistry of the coordination compounds, they more closely resemble the alkaline earth metals than the d-type transition metals in forming coordination compounds. The predominant factor in forming lanthanide complexes is believed to be the electrostatic interaction of the lanthanide ion with the ligand, which may either be an anion or a dipole in a molecule. The contribution of the f orbitals for metal-ligand orbital interaction compared to the contribution of the d orbitals is very small as evidenced by the fact that the lanthanide complexes have very little directional preference for bonding, ligands bond in order of electronegativity (23), and the spectra of the lanthanide ion is only slightly affected by the presence of coordinating ligands. The main controversies among researchers are:

1) What is the coordination number of the lanthanide ions?

2) Does the 20% decrease in ionic radius cause a change in the coordination number across the series?

3) If the coordination number of the lanthanides changes, at what point in the series does it change?

Statement of the Problem

This thesis deals directly with the questions:

1) Do solid complexes of lanthanide ions show a change in coordination number from early in the series, large ionic radius, to late in the series, small ionic radius?

2) What is the coordination number of a lanthanide ion early in the series and the coordination number of a lanthanide ion late in the series?

Dimethyl sulfoxide was used as the coordinating ligand due to the proven ability of dimethyl sulfoxide to form strong monodentate coordination compounds with metal ions (9,11,12,25,56,60).

Anhydrous salts of lanthanides were synthesized, the composition determined by chemical analysis, and the absence of water confirmed by Karl-Fischer titration.

Single crystals of the complexes were produced to insure homogeneous composition of the complex and a suitable morphology for x-ray studies.

Coordination of all the ligands present was confirmed by Raman and infrared spectroscopy. The molecular formula of the complexes was determined by chemical analysis.

CHAPTER II

SYNTHESIS AND ANALYSIS

Introduction

For x-ray analysis, it was necessary to synthesize complexes of the lanthanides that could be precipitated as single crystals. Various methods for producing single crystals of dimethyl sulfoxide were tried using several lanthanide ions and ClO_4^-, Cl^-, and Br^- as anions. Through trial and error, it was determined that complexes of dimethyl sulfoxide with praseodymium and holmium bromide were the only ones attempted that would consistently produce single crystals. Hence, this study is devoted to the synthesis and characterization of the dimethyl sulfoxide complexes of praseodymium and holmium bromides.

Preparation and Analysis of Anhydrous Bromides of Praseodymium and Holmium

The bromides of praseodymium and holmium were prepared by reacting the corresponding oxide, available from American Potash and Chemical Corporation, Rare Earth Division, Chicago, Illinois, with an aqueous solution of HBr, approximately 1 M. When all of the rare earth oxide had dissolved, the solution was filtered to remove any solid impurities and excess oxide. The filtrate was then heated on a hot plate at approximately $90^{\circ}C$ to remove the bulk of the water. The thick paste of rare earth bromide in hydrated form was dissolved in absolute ethanol and re-

fluxed over 4 Å Linde molecular sieve for 40 to 60 hours to remove the remaining water using a molecular sieve reflux extractor as described by Arthur, et al. (65). When a 50 cc sample indicated no water present by a Karl-Fischer titration (corresponding to a water content of less than 10 ppm), the excess ethanol was distilled off until the rare earth bromide just began to precipitate. The solution was transferred to a vacuum vessel and the remaining ethanol removed under vacuum to produce the solid anhydrous lanthanide bromide. The lanthanide bromides are very hydroscopic and all further work with the salt was performed in an inert atmosphere box as described by Eubanks and Abbott (66).

Samples of the anhydrous bromides were analyzed for lanthanide ion and bromide by transferring, in the inert atmosphere box, approximately 90 mg of the bromide to tared containers. The samples were then weighed to the nearest 0.1 mg and analyzed.

Lyle and Rahman (67) have compared methods for determination of lanthanides and concluded that the most satisfactory and convenient method for direct titration was to use EDTA with xylenol orange as an indicator at pH 5.8 to 6.4. The EDTA was prepared in aqueous solution and standardized against a zinc solution using zincon as an indicator.

The weighed samples were dissolved in water and buffered to pH 5.8 to 6.4 with an acetic acid-sodium acetate buffer. Three drops of xylenol orange indicator, 0.1% in H_2O and ethanol, was added along with one drop of pyridine, and titrated with the standard EDTA solution to the end point. As was pointed out by Lyle and Rahman (67), the end-point can be approached more rapidly if the solution is warmed. The titration was carried out using a 10 ml microburet calibrated in 0.02 ml divisions. The percentage lanthanide ion in each sample was calculated from Equa-

tion 1.

$$\% \, Ln^{3+} = \frac{(M \text{ EDTA}) \, (\text{ml EDTA})(\text{AW of } Ln^{3+}) \, (100)}{(\text{g sample}) \, (1000)} \qquad (1)$$

The results are summarized in Table III and Table IV.

The samples were analyzed for bromide by potentiometric titration and the results confirmed by weighing the precipitated bromide salt. Approximately 100 mg of the lanthanide bromide was weighed to the nearest 0.1 mg dissolved in 200 ml of water, and titrated potentiometrically using 0.0440 N standard $AgNO_3$ solution. The potential was measured using a Beckman Expandomatic SS-2 pH meter, a Corning Calomel reference electrode, and a Corning Triple Purpose Ag/AgCl electrode. The potentiometric end points were determined graphically and the percentage of bromide in the sample calculated from Equation 2. The potentiometric titration curves showed some deviation from ideal behavior, probably due to absorp-

$$\% \, Br^- = \frac{(N \, AgNO_3) \, (\text{ml } AgNO_3) \, (79.916) \, (100)}{(\text{g sample}) \, (1000)} \qquad (2)$$

tion of either Br^- or Ag^+ by the precipitate (68). The results were checked by gravimetric analysis of the AgBr. The solution from the potentiometric titration was acidified with nitric acid and three ml of the standard $AgNO_3$ solution was added. The solution was heated almost to boiling and digested at that temperature for 10 to 15 minutes. The solution was stored overnight in the dark and then filtered using a tared fritted-glass porcelain crucible. The precipitate was thoroughly washed with a dilute solution of nitric acid, dried to constant weight at 105° to 110°C, and weighed to the nearest 0.1 mg. The percentage of bromide in the sample was calculated from Equation 3. The results from the

TABLE III

COMPOSITION OF ANHYDROUS PRASEODYMIUM BROMIDES

Sample	% Pr	% Br
Theoretical for $PrBr_3$	37.02	62.98
Experimental		
1	37.00	
2	36.98	
3	37.04	
4	37.02	
5		63.01
6		62.94
7		62.98
8		63.02
Mean	37.01	62.99
Standard deviation	0.03	0.04

TABLE IV

COMPOSITION OF ANHYDROUS HOLMIUM BROMIDE

Sample	% Ho	% Br
Theoretical for $HoBr_3$	40.76	59.24
Experimental		
1	40.72	
2	40.78	
3	40.75	
4	40.82	
5		59.28
6		59.19
7		59.26
8		59.24
Mean	40.77	59.24
Standard deviation	0.04	0.04

gravimetric analysis and the results from the potentiometric analysis

$$\% \ Br^- = \frac{(g \ AgBr)\ (79.916)\ (100)}{(187.796)\ (g \ sample)} \qquad (3)$$

were in good agreement with the gravimetric results having the smaller variance. The experimental percentage of bromide in the samples is tabulated in Table III and Table IV. The mole ratio of lanthanide ion to bromide ion was found to be 0.2626:0.7882 or 1:3.001 for $Pr^{3+}:Br^-$ and 0.2472:0.7413 or 1:2.999 for $Ho^{3+}:Br^-$. The above ratios and the standard deviations listed in Table III and Table IV indicate that both praseodymium and holmium are in trivalent oxidation states.

Preparation of Dimethyl Sulfoxide Complexes

Various methods were attempted to produce single crystals of the complexes of the lanthanide bromides with dimethyl sulfoxide (DMSO). Complexes of lanthanide bromides with DMSO are easily prepared by dissolving an anhydrous lanthanide bromide in anhydrous methanol, then adding DMSO to precipitate the complex. The complex was reprecipitated by dissolving in a solution of 20% DMSO in acetonitrile and adding benzene to precipitate the complex. The solid produced consisted of very fine particles with none being identified as single crystals.

Numerous methods were attempted to produce single crystals of the complex. Three of the most successful methods were:

1) Solvent evaporation method - The complex was dissolved in excess acetonitrile and the acetonitrile allowed to slowly evaporate at room temperature under a stream of dry nitrogen to prevent absorption of water by the complex. The solid that formed was again composed of fine particles, as they were before recrystallization.

2) Vapor diffusion method - The complex was dissolved in acetonitrile and placed in a small beaker which in turn was placed in a larger beaker containing benzene and sealed. The diffusion of the benzene into the acetonitrile solution is very slow with solid first appearing after six to eight weeks. The solid was identical in appearance to the original complex and was unsatisfactory for x-ray study.

3) Vacuum removal of excess DMSO (60) - The anhydrous lanthanide bromide was dissolved in a large excess of DMSO. The excess DMSO was slowly removed on a high vacuum line (the vapor pressure of DMSO at 25°C is 0.8 torr) until solid began to appear. Solid was produced in the bottom of the vacuum vessel and also adhering to the side of the vessel at and above the solvent level. The solid adhering to the side of the vessel was shown by x-ray diffraction to be amorphous. The solid produced in the bottom was crystalline with well defined faces and edges indicating a large proportion of single crystals. Only the well defined crystals from the bottom of the vessel were used in this study. Single crystals of $PrBr_3 \cdot 8DMSO$ are transparent and light green in color. They tend to grow as needles up to 0.5 cm in length with monoclinic external symmetry.

Single crystals of $HoBr_3 \cdot 8DMSO$ are transparent and light yellow in color. They usually grow to form external cubic symmetry up to 1 cm in size. The $HoBr_3 \cdot 8DMSO$ crystals, if left in a container under the saturated solution will distort their symmetry to conform to the shape of the container.

Both complexes were highly unstable under normal atmospheric conditions. In order to determine how to prevent the decomposition, it was necessary to determine if the decomposition was due to atmospheric water

or oxygen. Samples of the two complexes weighing approximately 100 mg were crushed to the same consistency. Passing dry oxygen over the samples had no effect. However, when wet nitrogen was passed over the samples, both solids began to change to a liquid presumably by absorbing water and then dissolving. For the praseodymium complex, a surface of liquid was observed to form on the solid within a few seconds after the sample was exposed to wet nitrogen and within 15 minutes all that remained was a green liquid. Decomposition of the holmium complex was much slower and required 50 minutes until only liquid remained. All further transfers were performed in the dry box. It was noted that even in an inert atmosphere, both complexes had a tendency to fog and eventually form cracks in the crystals.

The synthesis and crystal growing techniques were also applied to systems of Cl^- and ClO_4^- salts of lanthanum, cerium, neodymium, samarium, gadolinium, dysprosium, erbium, and lutetium with DMSO. In all cases the solid produced did not contain single crystals.

Analysis of Dimethyl Sulfoxide Complexes of Lanthanide Bromides

The complexes were analyzed for bromide and lanthanide ion using the same procedures and relationships described for analysis of the rare earth bromides. The results are listed in Table V and Table VI.

DMSO is oxidized to dimethyl sulfone by $KMnO_4$ (69). However, the $KMnO_4$ is reduced only to MnO_2 and Fe^{2+} was added to complete the reduction to Mn^{2+}. The bromide present in the complex would also react with the $KMnO_4$ and must be removed prior to addition of $KMnO_4$. DMSO is thermally stable in acidic solution, except under conditions of prolong-

TABLE V

COMPOSITION OF PRASEODYMIUM COMPLEX

Sample	% Pr^{3+}	% Br^{-}	% DMSO
1	14.09		
2	13.90		
3	14.10		
4	14.01		
5		24.47	62.12
6		24.14	62.14
7		23.85	62.21
8		23.78	62.13
Mean	14.03	24.06	62.15
Standard Deviation	0.09	0.31	0.04

TABLE VI

COMPOSITION OF HOLMIUM COMPLEX

Sample	% Ho^{3+}	% Br^-	% DMSO
1	15.78		
2	16.00		
3	16.12		
4	16.04		
5		22.67	60.71
6		23.03	60.71
7		23.46	60.69
8		23.27	60.69
Mean	15.99	23.11	60.70
Standard Deviation	0.14	0.34	0.01

ed refluxing at 100°C (70). The filtrate from the bromide analysis showed no signs of thermal decomposition of the DMSO, characteristically an odor due to trace amounts of methyl mercaptan and bimethylthiomethane (70), and yielded excellent results for the analysis of DMSO.

$KMnO_4$ solution was prepared and standardized against primary-standard sodium oxalate as described by Skoog and West (68). The standardization yielded a normality of 0.108 N $KMnO_4$ for a five-electron change. The Fe^{2+} solution was prepared by dissolving $Fe(NH_4)_2(SO_4)_2 \cdot 6H_2O$ in water. The iron solution was standardized just prior to the DMSO analysis by titration against the standard $KMnO_4$ solution and found to be 0.0980 N.

To the filtrate from the bromide analysis, 25 ml of concentrated sulfuric acid, 25 ml of the standard $KMnO_4$ solution, and enough water to give a total volume of 300 ml were added to yield dimethyl sulfone and MnO_2 as described by the following reactions:

$$(CH_3)_2SO + H_2O \rightarrow (CH_3)_2SO_2 + 2H^+ + 2e^-$$
$$MnO_4^- + 4H^+ + 3e^- \rightarrow MnO_2 + 2H_2O$$
$$3(CH_3)_2SO + 2MnO_4^- + 2H^+ \rightarrow 3(CH_3)_2SO_2 + H_2O + 2MnO_2$$

Twenty-five ml of the standard Fe^{2+} solution was added to complete the reduction of $KMnO_4$:

$$MnO_2 + 4H^+ + 2e^- \rightarrow Mn^{2+} + 2H_2O$$
$$Fe^{2+} \rightarrow Fe^{3+} + e^-$$
$$2Fe^{2+} + MnO_2 + 4H^+ \rightarrow 2Fe^{3+} + Mn^{2+} + 2H_2O$$

The excess Fe^{2+} was then titrated to the end point with the standard $KMnO_4$ using a microburet:

$$Fe^{2+} \rightarrow Fe^{3+} + e^-$$

$$MnO_4^- + 8H^+ + 5e^- \rightarrow Mn^{2+} + 4H_2O$$

$$5Fe^{2+} + MnO_4^- + 8H^+ \rightarrow 5Fe^{3+} + Mn^{2+} + 4H_2O$$

All of the MnO_4^- was eventually reduced to Mn^{2+} so the intermediate MnO_2 need not be considered. The percentage of DMSO in the sample was calculated from Equation 4.

$$\% \text{ DMSO} = \frac{78.133\ [(\text{total ml } KMnO_4)(N\ KMnO_4) - (\text{ml } Fe^{2+})(N\ Fe^{2+})](100)}{(2)\ (1000)\ (\text{g sample})} \quad (4)$$

The results of the DMSO analysis are listed in Table V and Table VI.

The theoretical percentage compositions of praseodymium complexes with varying numbers of DMSO molecules, n_1, are tabulated in Table VII. The theoretical composition of holmium complexes with varying DMSO content, n_2, are tabulated in Table VIII. Comparing the experimentally determined percentage compositions of the praseodymium and holmium complexes, Tables V and VI respectively, to the idealized values listed in Table VII and Table VIII, it was apparent that both of the solid complexes contained lanthanide, bromide, and DMSO in a ratio of 1:3:8 respectively and n_1 and n_2 both have a value of eight.

A statistical treatment of n_1 and n_2 was achieved by randomly associating the experimentally determined compositions for the three components to yield four sets of complete analysis data for each complex and calculating values of n_1 and n_2 (71). More than four sets of compositions for each complex could have been generated but this would produce misleading statistical results since only four samples were used to determine the percentage of each component in each complex. To maintain charge balance in the complex, the ratio of lanthanide ion to bromide

TABLE VII

IDEALIZED COMPOSITION OF PRASEODYMIUM COMPLEX

n_1	Molecular Formula	Molecular Weight	% Pr^{3+}	% Br^-	% DMSO
0	$PrBr_3$	380.668	37.02	62.98	0
1	$PrBr_3 \cdot DMSO$	458.804	30.71	52.25	17.03
2	$PrBr_3 \cdot 2DMSO$	536.940	26.24	44.65	29.10
3	$PrBr_3 \cdot 3DMSO$	615.076	22.91	38.98	38.11
4	$PrBr_3 \cdot 4DMSO$	693.212	20.33	34.59	45.09
5	$PrBr_3 \cdot 5DMSO$	771.348	18.27	31.08	50.65
6	$PrBr_3 \cdot 6DMSO$	849.484	16.59	28.22	55.19
7	$PrBr_3 \cdot 7DMSO$	927.620	15.19	25.85	58.96
8	$PrBr_3 \cdot 8DMSO$	1005.756	14.01	23.84	62.15
9	$PrBr_3 \cdot 9DMSO$	1083.892	13.00	22.12	64.88
10	$PrBr_3 \cdot 10DMSO$	1162.028	12.13	20.63	67.24

TABLE VIII

IDEALIZED COMPOSITION OF HOLMIUM COMPLEXES

n_2	Molecular Formula	Molecular Weight	% Ho^{3+}	% Br^-	% DMSO
0	$HoBr_3$	404.688	40.76	59.24	0
1	$HoBr_3 \cdot DMSO$	482.824	34.16	49.66	16.18
2	$HoBr_3 \cdot 2DMSO$	560.960	29.40	42.74	27.86
3	$HoBr_3 \cdot 3DMSO$	639.096	25.81	37.51	36.68
4	$HoBr_3 \cdot 4DMSO$	717.232	22.99	33.43	43.58
5	$HoBr_3 \cdot 5DMSO$	795.368	20.74	30.14	49.12
6	$HoBr_3 \cdot 6DMSO$	873.504	18.88	27.45	53.67
7	$HoBr_3 \cdot 7DMSO$	951.640	17.34	25.19	57.47
8	$HoBr_3 \cdot 8DMSO$	1029.776	16.02	23.28	60.70
9	$HoBr_3 \cdot 9DMSO$	1107.912	14.89	21.64	63.47
10	$HoBr_3 \cdot 10DMSO$	1186.048	13.92	20.30	65.86

ion must be 1:3 as in the anhydrous lanthanide bromide. No steps were taken in the synthesis of the complexes that would have produced a change in the oxidation state of the lanthanide ion. Tables IX and X list the random compositions used and the calculated values of n_1 and n_2. A confidence interval for the values of n_1 and n_2 was determined by assuming a normal distribution for experimental values of n_1 and n_2. For samples from a normal distribution for which the population mean, μ, and the population variance, σ^2, are unknown, the sample mean, $\bar{X}$, and the sample variance, s^2, are used as estimators for μ and σ^2 respectively based on n-1 degrees of freedom (72). For a normal distribution of n_1 or n_2, the variable defined by Equation 5 has a t_{n-1} distribution. $\bar{X}$ is the calculated mean for n_1 or n_2 and μ is the true mean. The sample size n is 4 and s is the calculated standard deviation. The limits of the confidence interval are $\bar{X}-cs/\sqrt{n}$ and $\bar{X}+cs/\sqrt{n}$ where c is determined from tabulated values for "Student's t distribution" (72) based on the degrees of freedom, n-1, and the selected significance level. At a significance level of 0.05 (i.e., the probability of μ being within the confidence interval is 0.95) the following limits for the confidence intervals were determined:

$$T = \frac{\bar{X} - \mu}{s/\sqrt{n}} \qquad (5)$$

For n_1 based on the ratio of DMSO to Pr^{3+}:

$$0.95 = P(7.912 < n_1 < 8.078)$$

For n_1 based on the ratio of DMSO to 3 Br^-:

$$0.95 = P(7.758 < n_1 < 8.096)$$

For n_2 based on the ratio of DMSO to Ho^{3+}:

TABLE IX

VALUES FOR n_1 BASED ON RANDOM SAMPLING OF PERCENT COMPOSITION OF PRASEODYMIUM COMPLEX

% Pr^{3+}	% Br^-	% DMSO	Mole Ratio Pr^{3+} : Br^- : DMSO	n_1 based on Pr^{3+}	n_1 based on $3Br^-$
14.09	24.47	62.12	0.0999:0.3063:0.7950	7.958	7.789
13.90	24.14	62.14	0.0986:0.3021:0.7953	8.066	7.898
14.10	23.85	62.21	0.1001:0.2984:0.7962	7.954	8.005
14.01	23.78	62.13	0.0994:0.2976:0.7952	8.000	8.016
			Mean	7.995	7.927
			Standard Deviation	0.052	0.106

TABLE X

VALUES FOR n_2 BASED ON RANDOM SAMPLING OF PERCENT COMPOSITION OF HOLMIUM COMPLEX

% Ho^{3+}	% Br^-	% DMSO	Mole Ratio Ho^{3+} : Br^- : DMSO	n_2 based on Ho^{3+}	n_2 based on $3Br^-$
15.78	22.67	60.71	0.0957:0.2837:0.7770	8.119	8.216
16.00	23.03	60.71	0.0970:0.2882:0.7770	8.010	8.088
16.12	23.46	60.69	0.0977:0.2936:0.7767	7.950	7.936
16.04	23.27	60.69	0.0972:0.2912:0.7767	7.991	8.002
			Mean	8.018	8.061
			Standard Deviation	0.072	0.121

$$0.95 = P(7.903 < n_2 < 8.132)$$

For n_2 based on the ratio of DMSO to 3 Br^-:

$$0.95 = P(7.868 < n_2 < 8.253).$$

The confidence intervals completely eliminated the possibility of praseodymium or holmium being complexed with more or less than eight DMSO molecules assuming all of the molecules present by analysis are coordinated to the lanthanide ion.

Molecular Weight Measurements

The results of the infrared and Raman study, Chapter IV, show that all of the DMSO molecules are coordinated. However, no information about the coordination of the bromide ions was available. While it is not practical to make assumptions about the coordination in solution versus the coordination in the solid, solution measurements such as conductance have been used to assign the coordination sphere for many lanthanide complexes (29,56,57,60). The halide ions I^-, Br^-, and Cl^- have all been found to form predominately outer-sphere complexes with lanthanide ions (73,74). By comparing the molecular weights based on chemical analysis to the experimentally determined molecular weights, the number of particles in solution was determined.

A Hitachi-Perkin-Elmer Model 115 Molecular Weight Apparatus was used for the molecular weight measurements. The only suitable solvent, i.e., compatible with the instrument and able to dissolve the complexes without reacting, was acetonitrile. For accurate measurements, the solvent must be anyhdrous. Reagent grade acetonitrile was dried over calcium hydride for several days and then distilled. Care was taken to prevent absorption of water from the atmosphere by acetonitrile.

The molecular weight apparatus functions on the principle that impurities in a solvent cause a lowering of the vapor pressure. A drop of solvent and a drop of solution at the same temperature are placed in a sealed container which is saturated with solvent vapor. Since the solution has a lower vapor pressure, solvent vapor will condense in the solution and the latent heat of vaporization will be discharged by the solvent. This creates a temperature rise in the solution until the solution and the reference solvent have the same vapor pressure. This temperature rise is measured by a thermistor. The instrument reading, ΔR, plotted against the molal concentration of the solution will yield a linear plot with a zero intercept. A non-zero intercept usually indicates the presence of water either in the solvent or in the sample cell. Corrections for a non-zero intercept can be made by translation of the plot of ΔR versus the molal concentration to zero. The amount of translation is then either added to or subtracted from the sample concentrations (75).

A calibration curve for the apparatus was made using benzil in acetonitrile. The benzil was recrystallized from ethanol prior to use. The molecular weight apparatus gives the best results in the range of 10^{-2} to 10^{-4} molal. The first trial yielded a plot with a zero ΔR reading corresponding to a concentration of -0.93×10^{-3} molal. The translation corrections were made and the molecular weights for the praseodymium and the holmium complexes calculated to be 106.4 and 108.9 respectively. This corresponded to $HoBr_3 \cdot 8DMSO$ and $PrBr_3 \cdot 8DMSO$ both dissociating to produce 9.45 particles per mole. The non-zero intercept of the plot of ΔR versus the molal concentration indicated the presence of water (133). The water present was apparently displacing DMSO from the coordination sphere of the lanthanide ion. This type of behavior was

also observed by following the decomposition of the solid complexes by exposing them to the atmosphere (Chapter III).

For the second trial, all solutions were redried and the sample cells filled in the inert atmosphere box. A zero intercept was obtained for the plot of ΔR versus the molal concentration. The molecular weights were calculated and found to be 257.2 and 263.4 for the praseodymium and holmium complexes respectively. Both molecular weights corresponded to dissociation of the complexes to form 3.91 particles per mole of complex. The deviation from an ideal value of 4.0 suggests a small amount of ion pairing in solution. However, it was of particular significance to note that both complexes behave in an identical manner. Based on the molecular weight measurements, all three bromide ions are probably not in the inner coordination sphere of $PrBr_3 \cdot 8DMSO$ and $HoBr_3 \cdot 8DMSO$.

Conclusions From Analytical Results

Since DMSO is a monodentate ligand and the crystals were assumed to be homogeneous, n_1 and n_2 should have integer values. Based on the confidence intervals for n_1 and n_2, it was concluded that both n_1 and n_2 have a value of eight and the complexes are represented by the formula $PrBr_3 \cdot 8DMSO$ and $HoBr_3 \cdot 8DMSO$.

The analytical results established the composition of the solid complex as being $PrBr_3 \cdot 8DMSO$ and $HoBr_3 \cdot 8DMSO$. There are numerous reports in the literature for analysis of praseodymium complexes. Reported coordination numbers for praseodymium and holmium complexes vary from six to nine. However, the papers which reported analysis results for the lanthanide ions (22,29,30,31,34.45,47,52,57,64,76,77,78) showed results with a larger deviation between the experimental percentage of lanthanide

ion and the ideal value for the complex formula assumed than were found in this research. Literature values are typically on the order of 0.1% low for lanthanide. The analysis for lanthanide · DMSO complexes in the literature (30,34,45,52) also show a larger deviation from the ideal value than do those reported in this research. The previously reported values for percentage of DMSO in lanthanide complexes are typically 0.4% higher than the ideal values. None of the cited references report a standard deviation for their analysis or a confidence interval for the coordination number. The poor agreement between experimental and ideal values in the literature could probably be decreased by using single or near single crystals of the complex for analysis as was done in this work. The trend in the literature values of high results for DMSO and low results for praseodymium or holmium could be explained in terms of the presence of a small fraction of uncoordinated DMSO molecules.

The results described in this chapter demonstrated that, with a small probability of error, the complexes could be written as having the composition $PrBr_3 \cdot 8DMSO$ and $HoBr_3 \cdot 8DMSO$. Infrared and Raman data (Chapter III) confirm that all eight of the DMSO molecules are coordinated and x-ray studies (Chapter IV) show that the complexes have very similar crystal structures. The molecular weight data indicates an analagous behavior for both complexes and that the three bromide ions are most likely not in the inner coordination sphere of the lanthanide ion.

CHAPTER III

RAMAN AND INFRARED STUDIES

Introduction

Many of the vibrational modes of molecules may be monitored by infrared and Raman spectroscopy. Molecular vibrations which cause a change in the dipole moment of the molecule are infrared active. The Raman active modes are those which create a change in the polarizability of the molecule (6,79,80,81,82,83).

Raman and infrared studies have proved very useful in studying complexes of metal ions (5,6,7,11,30,34,45,52,56,60,73). By monitoring the vibrational frequencies of the ligand, three basic changes in the vibrational spectra may be followed or noted (84,85):

1) Shift in Band Position - When a ligand coordinates with a metal ion, the vibrational modes are shifted to higher or lower frequencies than are observed for the uncoordinated ligand (84,85). For complexes with DMSO, the vibrational modes have been observed to usually shift to higher frequencies with the exception of the S=O stretch. The S=O stretching mode shifts to lower frequencies and has led researchers to conclude that DMSO coordinates with metal ions through oxygen (11,12,34, 45,52,56,60,86).

2) Changes in Band Intensities or Occurrence of New Bands - Changes in band intensities have been used to predict geometries of metal carbonyls and have only rarely been applied to other systems (84). Of more

interest is the appearance of new bands. Metal ligand stretching modes are the most frequent new bands to appear and are frequently used to reflect coordination symmetry. Coordination usually reduces the effective symmetry of the ligand and therefore changes the selection rules for the ligand.

3) Splitting in Ligand Bands - If the symmetry of the ligand is lowered upon coordination, bands that were degenerate in the free ligand may split. Also, if the spectrum of the solid is recorded the ligand vibrations may couple to produce lattice vibrations. For complexes of DMSO, many of the bands are broadened and this may be due to lattice vibrations arising from coupled ligand vibrations of DMSO.

This research represents the first application of Raman spectroscopy to the study of coordination compounds of DMSO with the lanthanides.

Raman Spectra

A high-resolution laser Raman spectrometer was readily available and was used to obtain spectral data. The Raman apparatus used was built by J. P. Devlin and his research group at Oklahoma State University. The apparatus was built from commercially available components and was the same apparatus as described by Smith (87). The laser excitation source was a Model 52 argon ion laser built by Coherent Radiation Laboratories. Other major components are a Hamner photon counting system, an FW-130 Photo-multiplier tube, and a Jarrell-Ash 25-100 dual monochromator.

Samples were prepared by sealing the complexes in 4-mm O.D. Pyrex tubes. The vibrational modes were excited by focusing the laser beam along the long axis of the sample tube. The anti-Stokes scattering was measured perpendicular to the laser beam. For all samples the excita-

tion source was the green line of the argon ion laser at 5145Å. To prevent decomposition of the samples, a minimum laser power was used. The laser had a tendency to tune itself at this setting making direct comparison of the band intensities impractical. The spectra were recorded by rapidly scanning, 100 cm^{-1} per chart division, the sample spectrum and then rescanning the observed bands at a slower, higher resolution setting, 20 cm^{-1} per chart division, to determine the band position.

The following samples were prepared and their Raman spectra recorded: pure DMSO, solid $PrBr_3 \cdot 8DMSO$, solid $HoBr_3 \cdot 8DMSO$, a saturated solution of $PrBr_3$ in DMSO, and a saturated solution of $HoBr_3$ in DMSO.

The Raman spectra of pure DMSO is shown in Figures 1 and 2. The observed frequencies are in excellent agreement with those reported in the literature (8,88,89,90,91,92). The saturated solutions of the bromides in DMSO either produced a broadening of the DMSO bands or the formation of two bands where only one was observed for pure DMSO. This indicated the presence of both coordinated and free DMSO molecules. Depolarization studies of the holmium solution show the same depolarization ratios as reported for pure DMSO (91). The Raman data for praseodymium bromide in DMSO did not yield a very satisfactory spectrum. The presence of a strong fluorescence band dominated throughout the spectrum. The unobscured bands of $PrBr_3$ in DMSO are shown in Figures 3 and 4. The Raman spectrum of $HoBr_3$ in DMSO is shown in Figures 5 and 6.

Raman spectra of the solid complexes yielded only frequencies that corresponded to coordinated DMSO. The bands were all shifted from those observed for pure DMSO. An additional band for each complex was observed between 80 and 90 cm^{-1}. These bands are somewhat obscured by a high background from the laser excitation line. These bands were assumed to

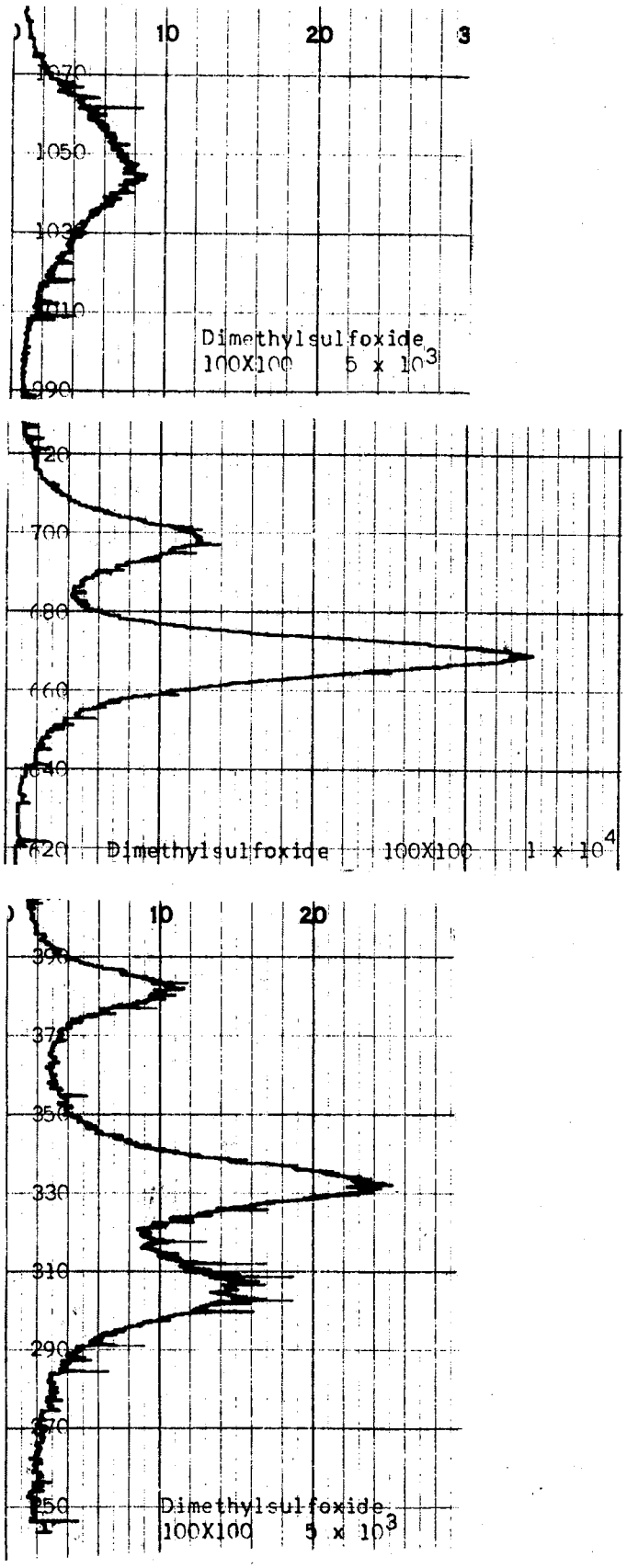

Figure 1. Raman Spectrum of Pure DMSO (250 cm^{-1} to 1090 cm^{-1})

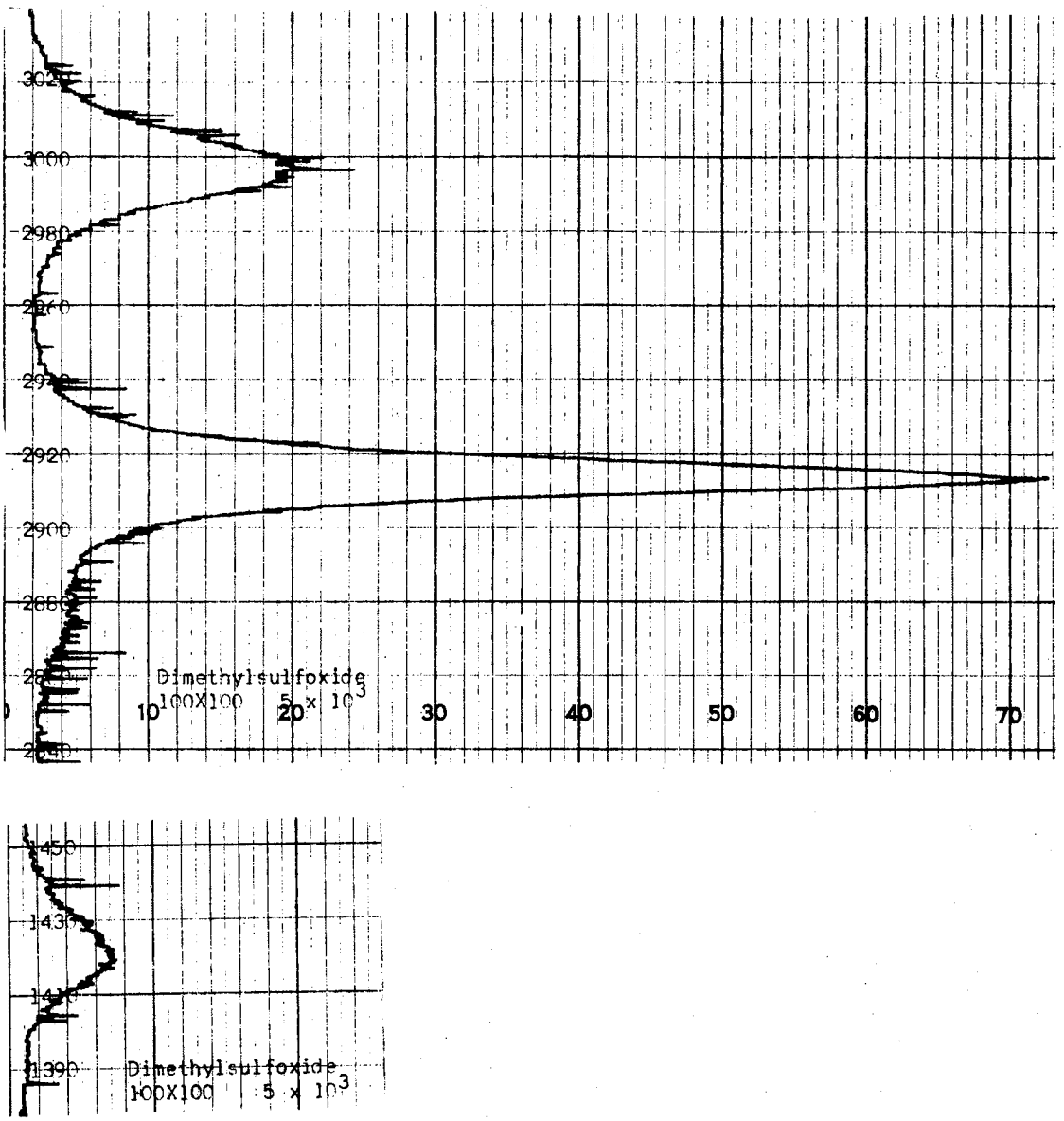

Figure 2. Raman Spectrum of Pure DMSO (1390 cm^{-1} to 3040 cm^{-1})

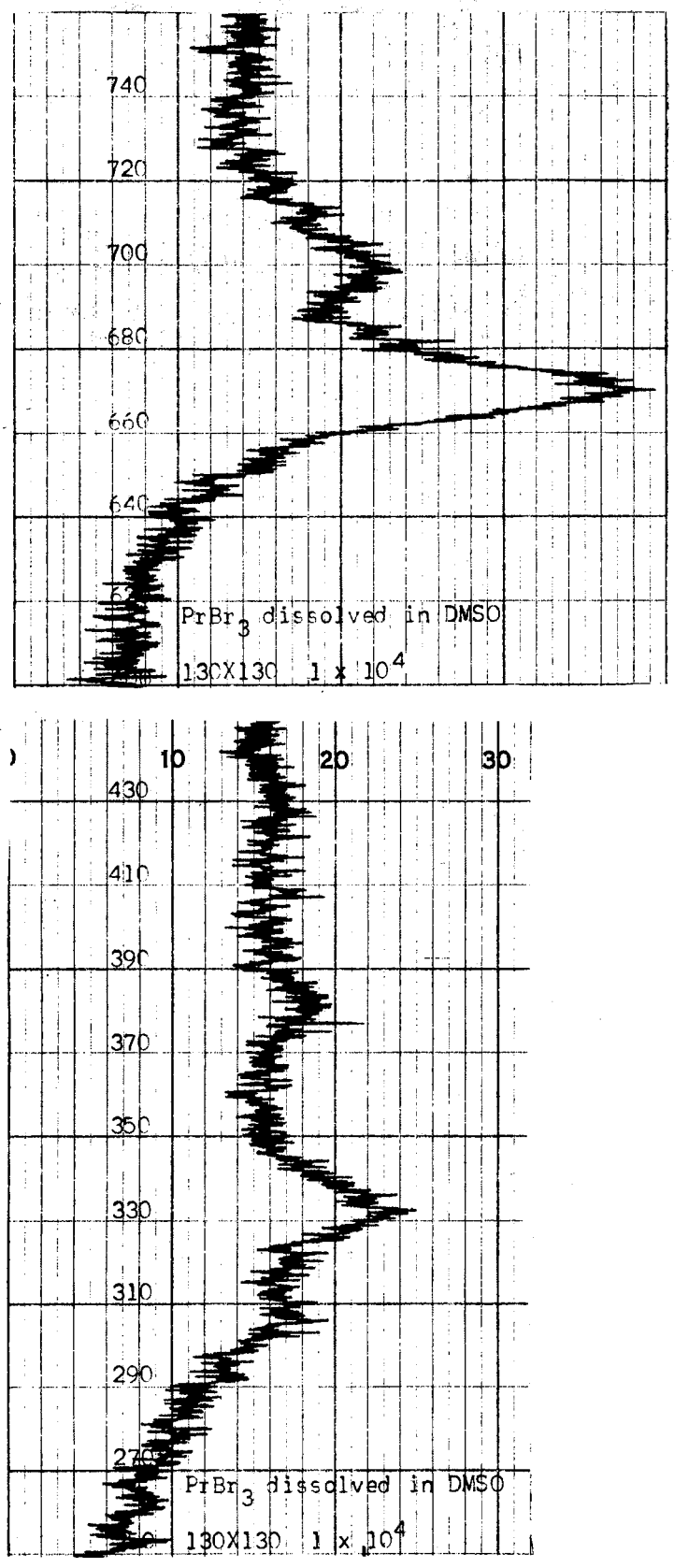

Figure 3. Raman Spectrum of $PrBr_3$ Dissolved in DMSO (250 cm^{-1} to 760 cm^{-1})

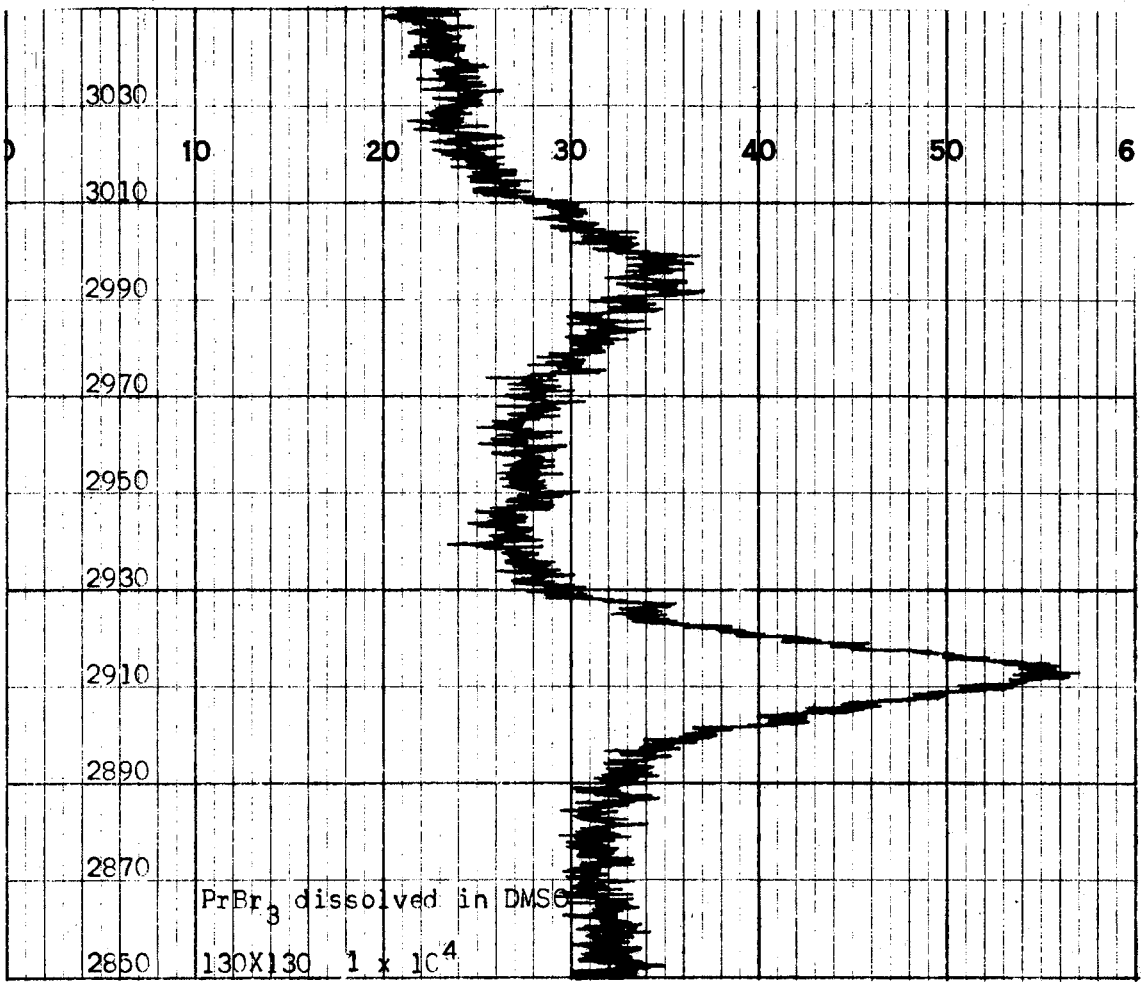

Figure 4. Raman Spectrum of $PrBr_3$ Dissolved in DMSO (2850 cm^{-1} to 3050 cm^{-1})

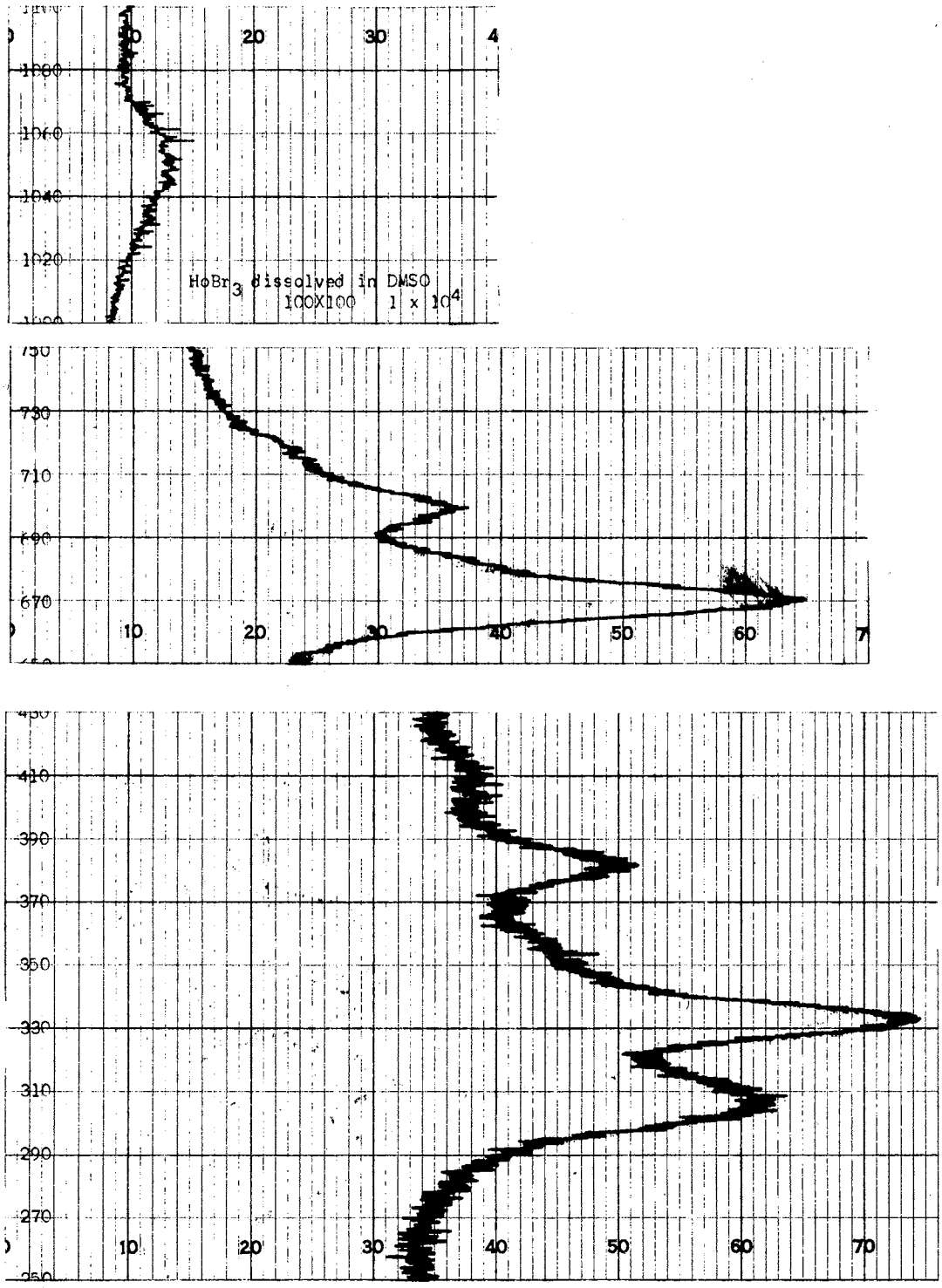

Figure 5. Raman Spectrum of $HoBr_3$ Dissolved in DMSO (250 cm^{-1} to 1100 cm^{-1})

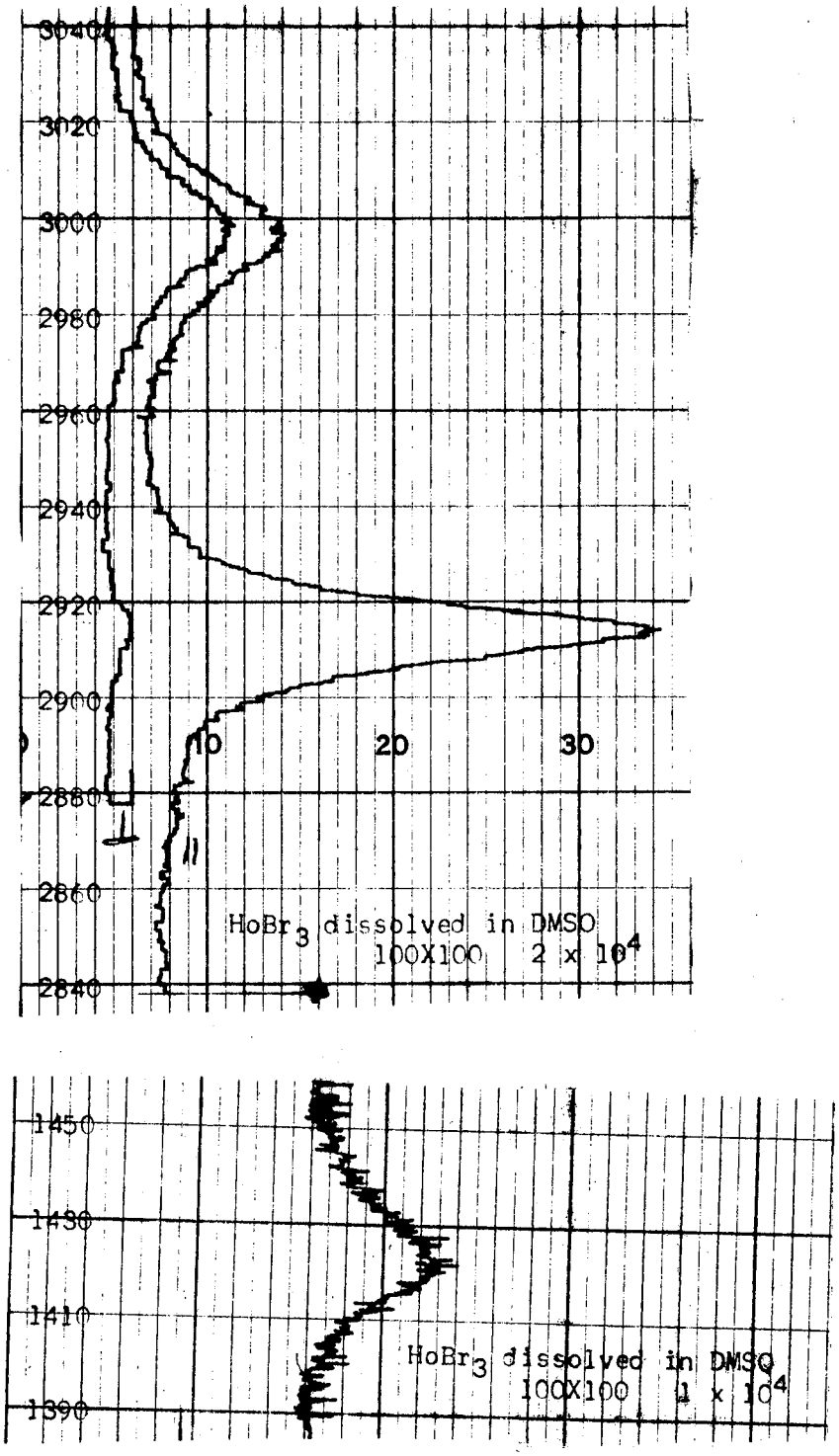

Figure 6. Raman Spectrum of $HoBr_3$ Dissolved in DMSO (1390 cm^{-1} to 3040 cm^{-1})

be due to a metal-oxygen stretching mode. The Raman spectra for the solid praseodymium and holmium complexes are shown in Figures 7 and 8 and Figures 9 and 10, respectively. The S=O stretching mode and vibrations due to water are not very active Raman modes and could better be observed by infrared spectroscopy.

Infrared Spectra

Infrared spectra were recorded to observe the Raman inactive bands. Of particular interest was the S=O band and infrared active water bands. The infrared spectra were recorded using a Beckman IR8 and a sodium chloride sample cell. The liquid samples were run as a thin film between the NaCl plates. The solid samples were recorded as mulls using mineral oil, fluorolube, and tetrachloroethylene as mulling agents. Attempts to prepare KBr pellet samples of the solid complexes were not successful. The pellets formed were always fogged and would not transmit enough light in the infrared to yield measureable spectra. This is believed to be due to interactions of the complex with KBr as suggested by other researchers (34).

None of the spectra indicated the presence of water in the sample. The spectra of the solid complexes showed a 40 to 50 cm^{-1} shift of the S=O frequency to about 1000 cm^{-1}. After the original spectra were recorded, the cells were opened to the atmosphere and the spectra recorded again. The spectra then contained very strong water bands and bands corresponding to both the coordinated and uncoordinated DMSO. Hence, the decomposition of the solid complexes as described in Chapter II was probably due to atmospheric water displacing DMSO in the coordination sphere of the lanthanide ion.

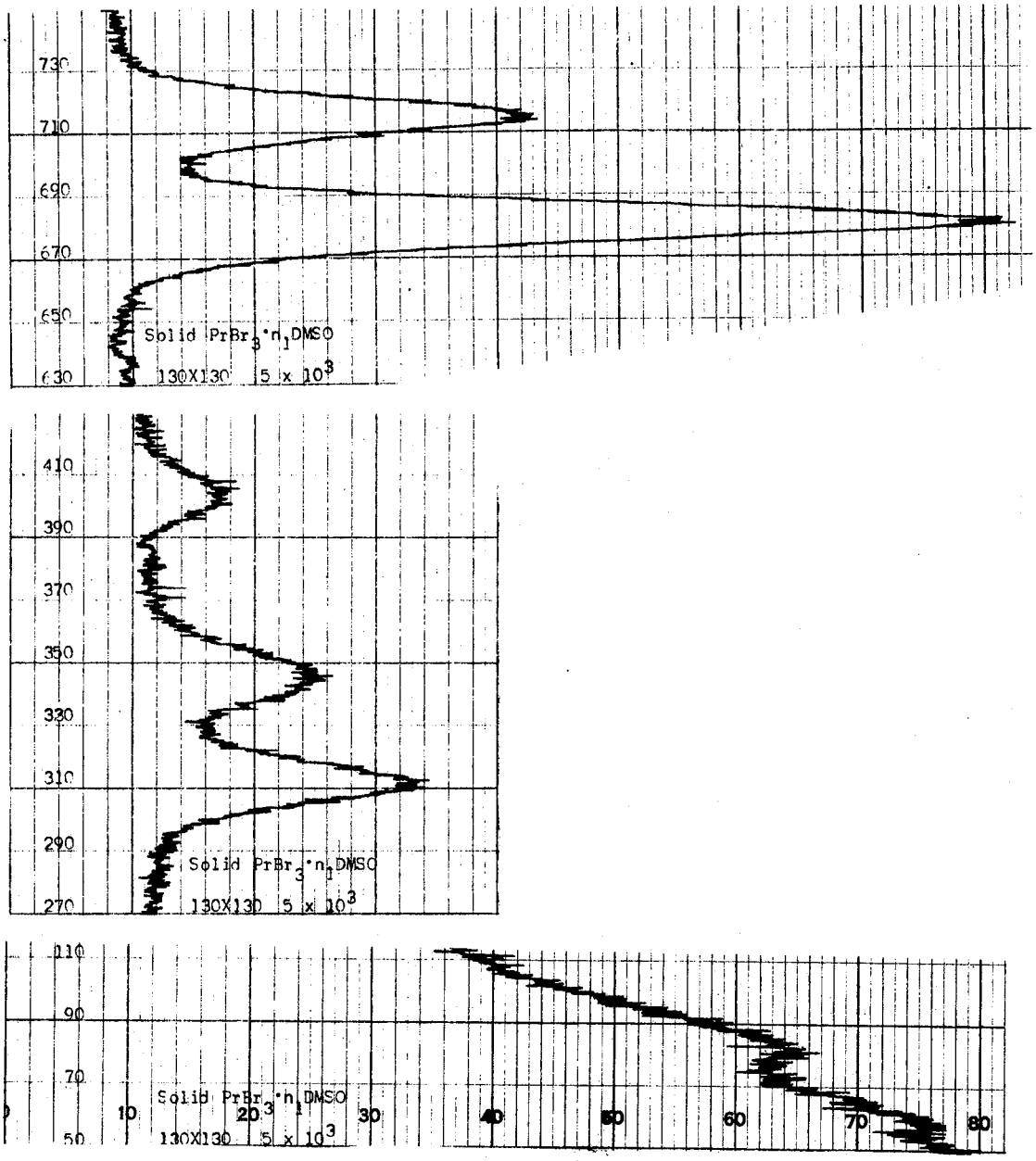

Figure 7. Raman Spectrum of Solid $PrBr_3 \cdot 8DMSO$ ($50\ cm^{-1}$ to $750\ cm^{-1}$)

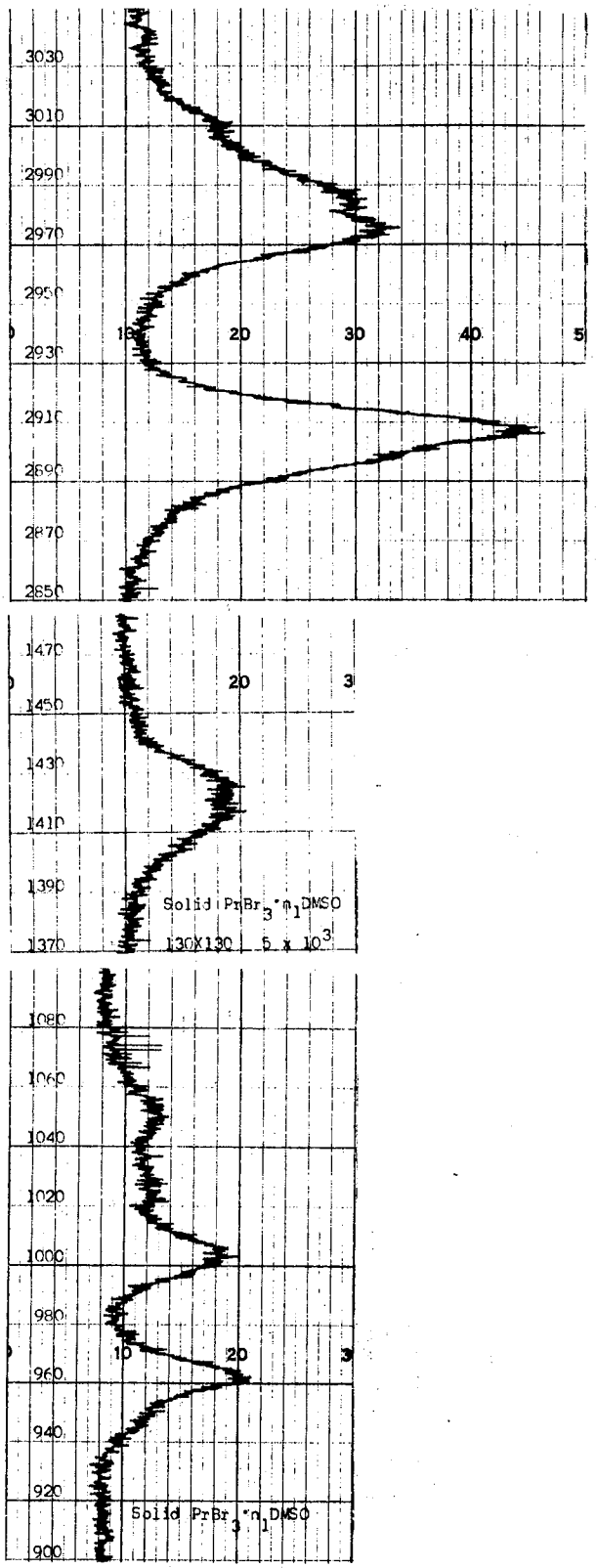

Figure 8. Raman Spectrum of Solid $PrBr_3 \cdot 8DMSO$ (900 cm^{-1} to 3050 cm^{-1})

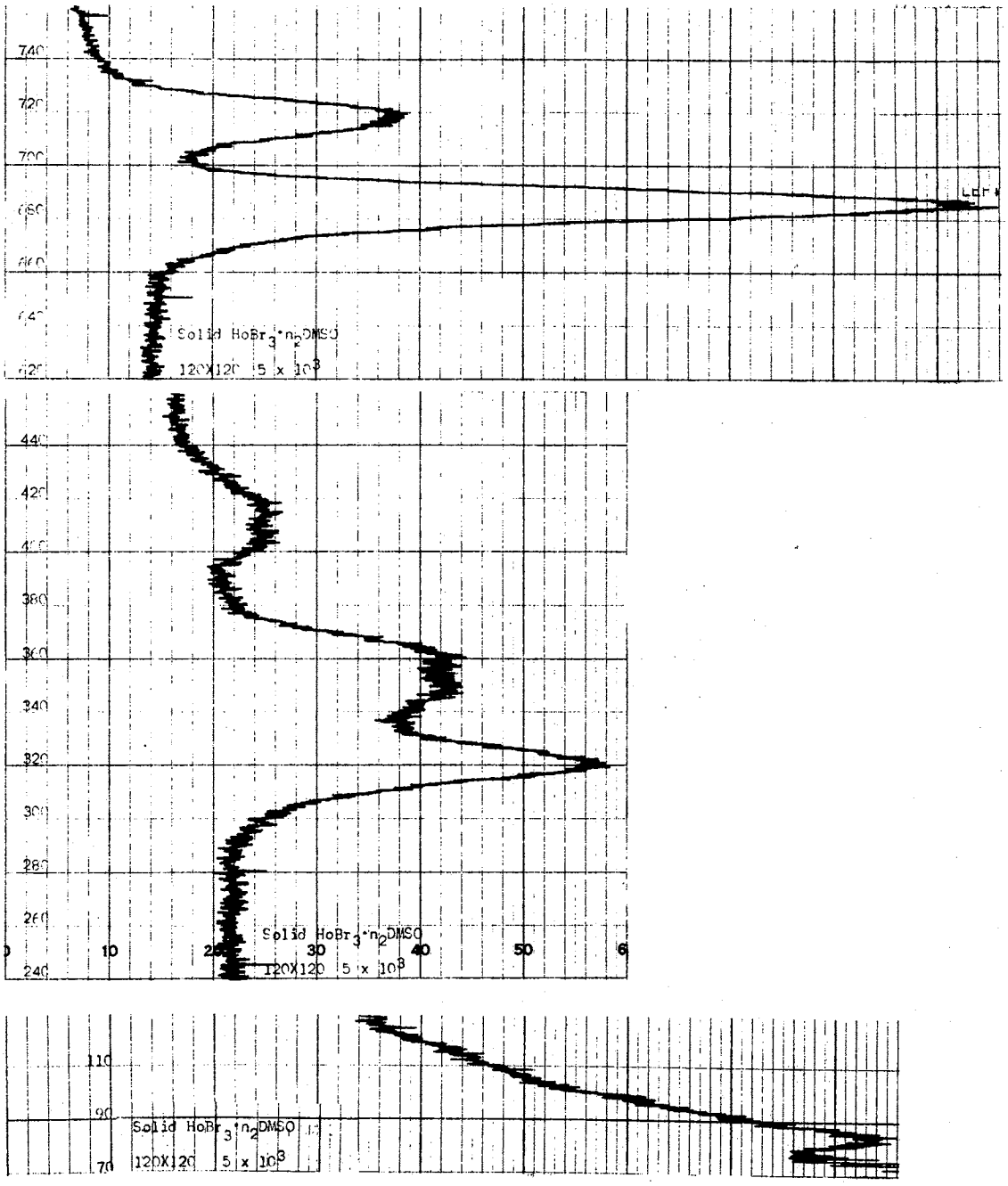

Figure 9. Raman Spectrum of Solid $HoBr_3 \cdot 8DMSO$ (70 cm^{-1} to 760 cm^{-1})

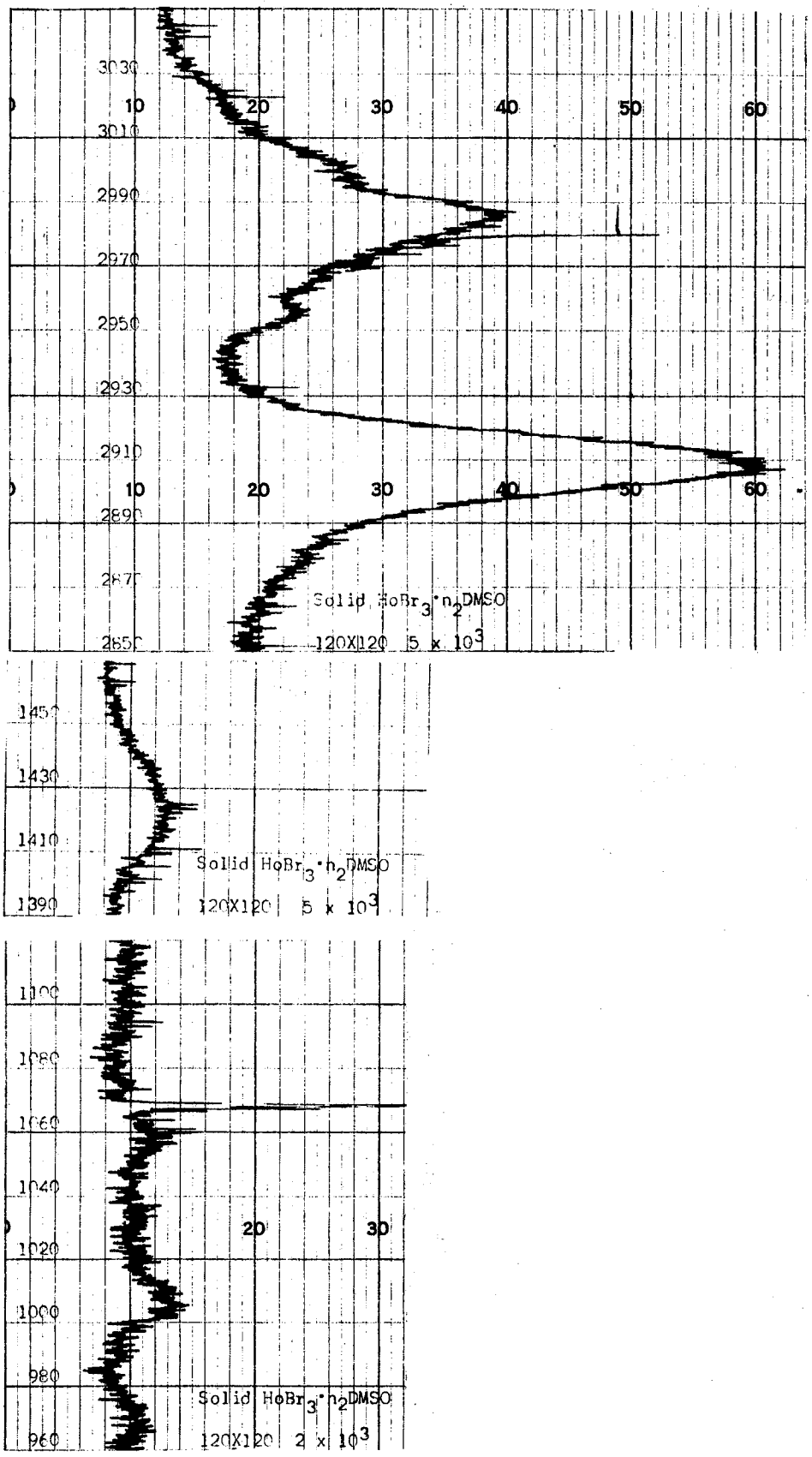

Figure 10. Raman Spectrum of Solid $HoBr_3 \cdot 8DMSO$ (960 cm^{-1} to 3050 cm^{-1})

Results and Conclusions From Spectra

The Raman and infrared spectra of the solid complexes showed definite shifts in the position of the DMSO bands when compared to the position of the uncoordinated DMSO bands. The observed bands and their assignments are tabulated in Table XI. Unless otherwise indicated, the band positions are those recorded by laser Raman spectroscopy. The band assignments were consistent with those found by other researchers (8,45, 52,88,90,92). Most of the bands showed an increase in frequency when the DMSO coordinates. The frequency of the SO stretching mode was of particular interest. Three resonance structures for DMSO have been proposed as shown in Figure 11 (11,30,34).

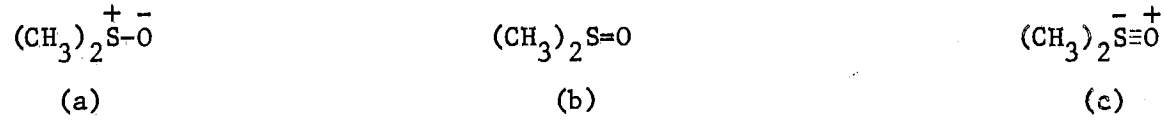

Figure 11. Structure of Dimethyl Sulfoxide

Structure (b) is predominant in free DMSO. When DMSO coordinates with a lanthanide ion, the contribution from structure (a) or (c) becomes more pronounced. If DMSO coordinates through O, the contribution of structure (a) increases, the SO bond order decreases, and the SO frequency is decreased. If DMSO coordinates through S, the SO bond order increases due to contributions from structure (c), and the SO frequency is increased (11,30,34). Experimental results showed a decrease in the SO frequency. Coordination of DMSO through oxygen was assumed. This was consistent with other reported results (30,32,86). X-ray studies on complexes of DMSO have also revealed coordination of DMSO through oxygen

TABLE XI

VIBRATIONAL FREQUENCIES OF DMSO COMPLEXES

Assignments	M-O Stretch	C-S-C Deformation	Antisymmetric C-S-O Deformation	Symmetric C-S-O Deformation	Symmetric C-S Stretch	Antisymmetric C-S Stretch	CH_3 Rocking
Ho^{3+}	86w	321m	350mb	408wb	686s	718m	970vw
Pr^{3+}	81w	312m	346m	404w	681s	714m	962w
DMSO		305m	332m	381w	669s	698m	950vw

Assignments	S=O Stretch	CH_3 Scissoring	C-H Stretch			
Ho^{3+}	1005s(ir)	1423w(ir)	2908m	2955	2986mb	3008sh
Pr^{3+}	1000s(ir)	1421w(ir)	2907m	2975mb	2985mb	3010sh
DMSO	1047s(ir)	1421w(ir)	2913m		2997m	

(25,46,93). Low frequency bands below 100 cm^{-1} were observed for both solid complexes and were assigned to M-O frequencies. Since all of the bands were shifted upon coordination and only slight band broadening was observed, it is believed that all of the ligands were equally coordinated to the metal ion. Some researchers have assigned the M-O frequency of lanthanide DMSO complexes to a band occurring at about 400 cm^{-1} (7,8, 30). However, Raman depolarization spectra show the same depolarization ratio of 0.42 for the 408 cm^{-1} band of $HoBr_3 \cdot 8DMSO$ and the 404 cm^{-1} band of $PrBr_3 \cdot 8DMSO$ as for the 381 cm^{-1} band of uncoordinated DMSO. As a result the bands in the region of 400 cm^{-1} were assigned to the symmetric C-S-O deformation rather than a M-O mode. The M-O mode was assigned to bands in the region of 80 to 90 cm^{-1}.

The DMSO bands were shifted the most for the holmium complex. This indicates that the DMSO molecules coordinate more strongly with holmium than with praseodymium. This can be rationalized by the increased charge density of holmium due to a decrease in ionic radius.

CHAPTER IV

X-RAY DIFFRACTION DATA

Introduction

Both single crystal and powder x-ray diffraction patterns were recorded. The powder patterns were used to verify that $PrBr_3 \cdot 8DMSO$ and $HoBr_3 \cdot 8DMSO$ have similar crystal structures. Weissenberg photographs of $PrBr_3 \cdot 8DMSO$ were made to verify that the complexes could be grown as single crystals. Cell constants for the reciprocal lattice were calculated. Both complexes showed a rapid rate of decomposition in the x-ray beam and a tendency toward absorption of the Cu K_α radiation. For this reason very precise measurements could not be made. A detailed description of the principles involved in x-ray crystallography and detailed derivations of the equations used may be found in any of the several books published on the study of crystals by x-ray diffraction (94,95,96, 97,98,99). Due to the tendency of $PrBr_3 \cdot 8DMSO$ and $HoBr_3 \cdot 8DMSO$ to decompose in normal atmospheric conditions, all sample manipulations were carried out in an inert atmosphere box.

Powder Method

Crystals of $PrBr_3 \cdot 8DMSO$ and $HoBr_3 \cdot 8DMSO$ with well defined faces were selected for the powder diffraction study. The selected crystals were ground to a fine powder using an agate mortar and pestle. The powdered samples were sealed in a glass capillary with an outside diameter of 0.2

mm. The glass capillaries were specially made for x-ray diffraction studies. Capillaries in a wide variety of diameters are readily obtained from numerous sources including General Rand Corporation and Charles Supper Company. The capillaries were sealed using an alpha cyanoacrylate cement. The cement is sold under the trade name of Zipbond by the Tescom Corporation. The cement polymerizes with trace amounts of surface moisture to form a solid seal. If the capillaries are thoroughly dry, the cement will remain fluid until removed from the inert atmosphere box and then solidify in less than ten seconds by absorbing water from the atmosphere. The sealed samples were placed in a Debye-Scherrer type camera (94,95,99). The camera has an internal diameter of 114.6 mm. A strip of x-ray film (Kodak NS-392T) was placed along the internal circumference of the camera as a detector. An x-ray beam was produced by a North American Philips Generator Type 12045/3 using a copper target. The beam was filtered through nickel foil to transmit only Cu K_α radiation, $\lambda = 1.54178$ Å. Generator settings of 25 KV and 15 ma were used. These settings are somewhat lower than those usually employed for x-ray diffraction studies. The lower settings were necessary to prevent rapid decomposition of the samples. As the sample was rotated in the x-ray beam, diffraction cones were produced when conditions for Bragg's Law, Equation 6, for x-ray diffraction were satisfied (96,99). Variables in

$$n\lambda = 2d \sin \theta \qquad (6)$$

Bragg's Law are the wavelength of the Cu K_α radiation, λ; the interplaner spacings in the crystal lattice, d; the angle of reflection and the angle of incidence, θ; and integral values of n.

The diffraction cones appear as symmetric arcs on the developed

film. The x-ray film was developed and dried and the distance between each pair of symmetric arcs measured to the nearest 0.05 mm using a North American Philips type 52022 film illuminator and measuring device. The geometry of the Debye-Scherrer camera is such that 2 mm on the undeveloped film corresponds to 1° of the Bragg angle θ. The usual procedure for measuring powder diffraction patterns is to correct for film shrinkage and errors in the camera diameter by measuring arcs in the back reflection region, $2\theta > 90^{\circ}$, and in the front reflection region, $2\theta < 90^{\circ}$, to determine the distance on the film between the entry point of the x-ray beam and the exit point of the undeflected x-ray beam. This value should correspond to 180° and a correction factor is applied if the value on the film is other than 180°. However, for compounds of praseodymium and holmium, no diffraction lines were observed in the back reflection region. An approximate correction factor was obtained by measuring the diffraction pattern of a sodium chloride sample using film from the same conditions as used for the praseodymium and holmium samples.

Powder samples of $PrBr_3$, $PrBr_3 \cdot 8DMSO$, $HoBr_3$, and $HoBr_3 \cdot 8DMSO$ were prepared and their diffraction patterns recorded. Optimum exposure times for the praseodymium and holmium samples were six and eight hours, respectively. All samples produced more than 20 diffraction cones in the region of $2\theta < 90^{\circ}$ and none beyond that region. As the diffraction cones approach 90°, the arcs become very weak and diffuse. The 20 most intense lines were measured for each sample. In all cases, the twenty most intense lines occur at values of 2θ less than 40°. As pointed out by Buerger (95) small errors in the measurement of 2θ in this region produce relatively large errors in the calculated values of d from Equa-

tion 6. Due to the above and problems in correcting for film shrinkage, the data obtained from the powder patterns were only approximate. The d values were obtained from the measured 2θ values by use of tables of interplaner spacings for copper radiation (100).

The values obtained from powder diffraction patterns of $PrBr_3$, Figure 12, and $HoBr_3$, Figure 13, were in good agreement with those reported in the literature (101). The values obtained from the powder diffraction patterns of $PrBr_3 \cdot 8DMSO$, Figure 14, and $HoBr_3 \cdot 8DMSO$, Figure 15, contained no diffraction arcs in common with the patterns for $PrBr_3$ and $HoBr_3$, respectively. Table XII contains the values obtained from the powder diffraction pattern of $PrBr_3 \cdot 8DMSO$, and those for $HoBr_3 \cdot 8DMSO$ are tabulated in Table XIII. The relative intensities were obtained visually by assigning a value of 1.0 to the most intense arc on each film and then comparing the relative intensity of the remaining arcs to the most intense.

The most significant result of the powder diffraction study was obtained by comparison of the calculated d spacings for the two complexes. Both complexes had very similar d spacings and the ratios between the calculated values of $\sin^2\theta$ show that the complexes have very similar crystal structures. The smaller d spacing for the holmium complex indicated a slightly smaller unit cell for $HoBr_3 \cdot 8DMSO$ than for $PrBr_3 \cdot 8DMSO$.

Weissenberg Photographs

The Weissenberg camera provides an indirect method of photographing the reciprocal lattice of a single crystal (95,96,97,98,99). The reciprocal lattice differs from the direct lattice in that the reciprocal lattice is defined by constructing normals to the direct lattice planes

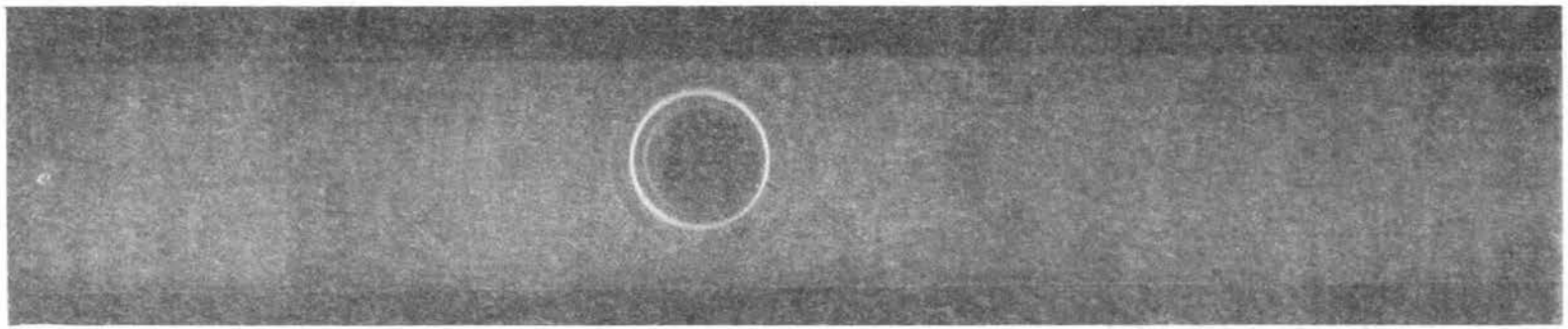

Figure 12. Powder Diffraction Pattern of $PrBr_3$

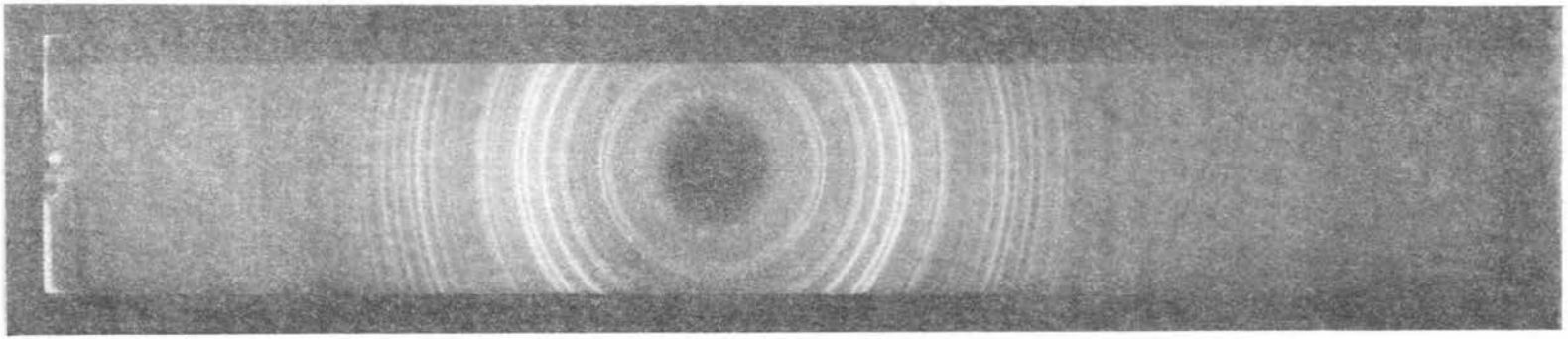

Figure 13. Powder Diffraction Pattern of $HoBr_3$

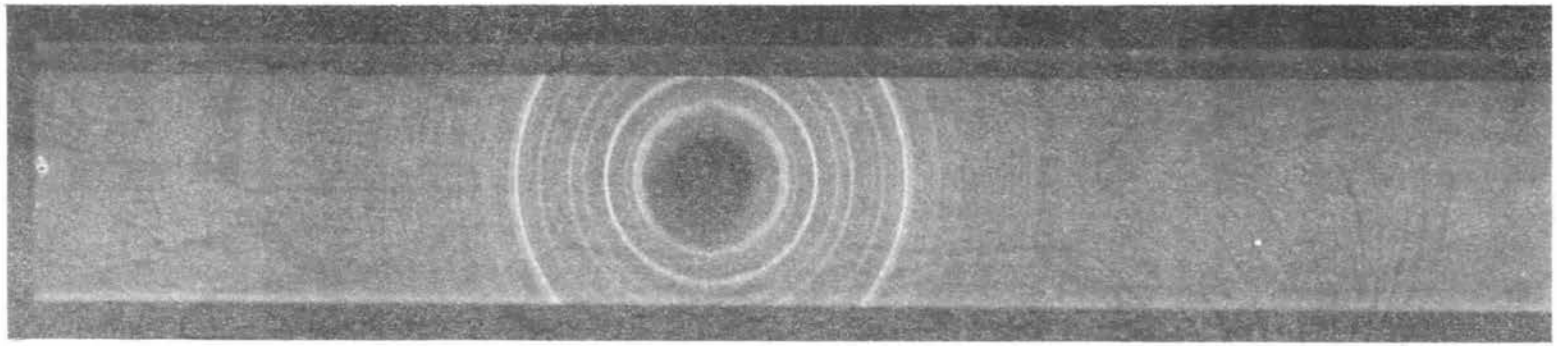

Figure 14. Powder Diffraction Pattern of $PrBr_3 \cdot 8DMSO$

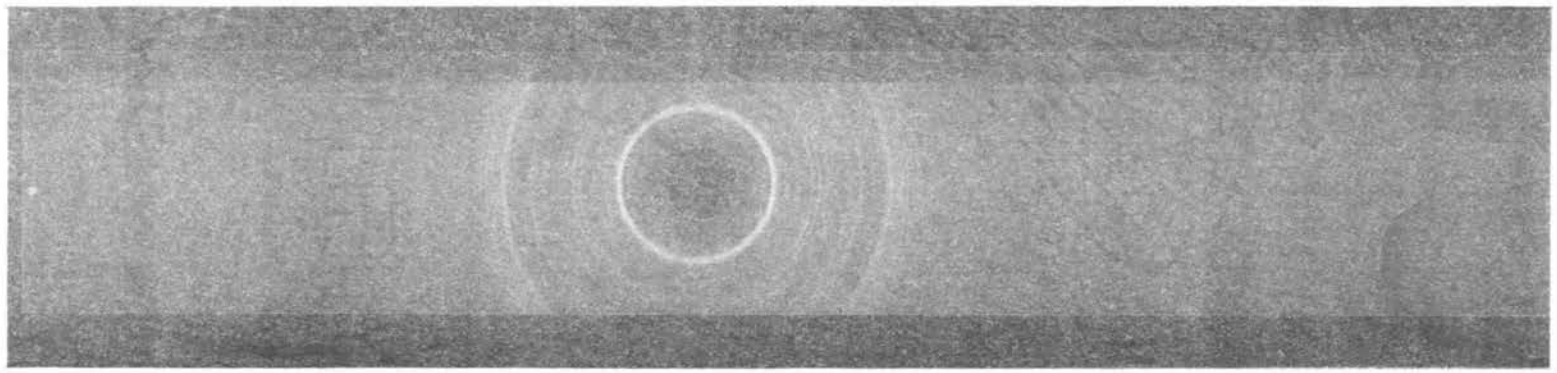

Figure 15. Powder Diffraction Pattern of $HoBr_3 \cdot 8DMSO$

TABLE XII

POWDER DIFFRACTION DATA FOR $PrBr_3 \cdot 8DMSO$

Line	2 θ	d	$\sin^2\theta$	Relative Intensity
1	9.05	9.77	0.0062	0.4
2	9.80	9.03	0.0073	0.5
3	11.00	8.04	0.0092	0.3
4	13.60	6.51	0.0140	1.0
5	16.30	5.44	0.0201	0.4
6	16.95	5.23	0.0218	0.1
7	18.15	4.89	0.0247	0.5
8	20.85	4.26	0.0326	0.3
9	22.10	4.02	0.0367	0.4
10	24.10	3.69	0.0436	0.1
11	24.95	3.57	0.0465	1.0
12	25.85	3.45	0.0502	0.2
13	27.10	3.29	0.0549	0.1
14	27.85	3.20	0.0581	0.1
15	28.60	7.12	0.0610	0.1
16	30.25	2.95	0.0679	0.1
17	31.80	2.81	0.0751	0.1
18	33.10	2.71	0.0811	0.1
19	34.45	2.60	0.0879	0.1
20	36.35	2.47	0.0970	0.1

TABLE XIII

POWDER DIFFRACTION DATA FOR $HoBr_3 \cdot 8DMSO$

Line	2 θ	d	$\sin^2\theta$	Relative Intensity
1	9.45	9.36	0.0067	0.8
2	10.25	8.63	0.0081	0.4
3	11.30	7.83	0.0097	0.5
4	13.95	6.35	0.0144	0.4
5	15.50	5.72	0.0182	0.4
6	16.50	5.37	0.0206	0.7
7	17.95	4.94	0.0239	0.1
8	18.90	4.70	0.0270	0.1
9	19.75	4.50	0.0293	0.1
10	21.25	4.18	0.0338	0.1
11	23.70	3.75	0.0422	1.0
12	24.90	3.58	0.0465	0.5
13	25.85	3.45	0.0502	0.4
14	27.00	3.30	0.0545	0.6
15	28.40	3.14	0.0602	0.6
16	30.75	2.91	0.0701	0.1
17	31.80	2.81	0.0751	0.2
18	33.05	2.71	0.0811	0.3
19	34.45	2.60	0.0874	0.2
20	36.00	2.49	0.0955	0.1

at the origin of the direct lattice. The length of the normals are $1/d_{hk\ell}$ where $d_{hk\ell}$ are the perpendicular distances between planes of the set (hkℓ). These normals define the edges of the reciprocal lattice (97). Relationships between the axis of the direct lattice, a, b, and c, and the axis of the reciprocal lattice, a*, b*, and c*, require that the crystal system be known. The crystal system and the reciprocal lattice constants were obtained by Weissenberg measurements.

The Weissenberg camera was manufactured by Charles Supper Company. The camera was designed to allow for either rotation or oscillation of a single crystal about an axis perpendicular to the impinging x-ray beam. The recording part of the camera consisted of a cylinder with an internal diameter of 57.3 mm lined with x-ray film (Kodak NS-54T). The radiation used was Cu K_α generated by the same system as described earlier for the powder method. The geometry of the camera was such that 1 mm on the film measured perpendicular to the axis of rotation corresponds to 1° of the Bragg angle, θ, defined by Equation 6.

For Weissenberg measurements, the ideal sample should be a spherically-shaped single crystal. However, equations for correcting for the shape of the crystal are available (96,97,98). Due to the absorption problem as described in the powder method, small crystals will yield the most accurate Weissenberg patterns. The crystals available of $PrBr_3 \cdot 8DMSO$ were smaller than those of $HoBr_3 \cdot 8DMSO$. Due to the above and the fact that holmium has an absorption edge, 1.5368 Å, close to the wavelength of the Cu K_α radiation, the crystals of $PrBr_3 \cdot 8DMSO$ were selected for the Weissenberg measurements. Based on the similar nature of the crystals of $PrBr_3 \cdot 8DMSO$ and $HoBr_3 \cdot 8DMSO$, it was assumed that crystals of $HoBr_3 \cdot 8DMSO$ would differ from those of $PrBr_3 \cdot 8DMSO$ only in having smaller

lattice dimensions.

Very little information has been published on techniques for mounting single crystals in an inert atmosphere box. Through trial and error, the following method was developed: numerous crystals that had been grown by vacuum removal of DMSO from a solution of $PrBr_3$ in DMSO were isolated from the saturated solution by filtration employing a glass frit and a rubber bulb aspirator. The crystals were washed and dried on the frit using benzene. The dried crystals were transferred to a petri dish by gently tapping the frit against the side of the petri dish. The crystals were examined optically using a telescope mounted outside the dry box. Crystals that appeared to have well defined faces, contained no visible fractures, and were less than 0.2 mm in the largest dimension were selected for mounting. Each crystal was transferred to a glass x-ray capillary tube. The capillary tubes were the same type as used for the powder samples. To obtain a more sensitive touch for transferring the small crystals to the capillary, the fingers were cut out of the standard dry box gloves, and surgical gloves were worn and inserted into the dry box gloves. A seal from the atmosphere was obtained by placing rubber bands around the wrist of the dry box gloves. The selected crystals were transferred one at a time to the capillary tubes by a nylon thread. It was found that the transfers were simplified if the nylon thread was first wetted by dipping the thread into the saturated solution of $PrBr_3$ in DMSO. The crystals would then adhere to the thread and could easily be picked up. To prevent gas currents from dislodging the crystal from the thread, it was necessary to turn off the recirculating mechanism of the inert atmosphere box. Each crystal was lodged in a tapered capillary tube by gently vibrating the tube with a triangu-

lar file. The capillary tubes were sealed using the alpha cyanoacrylate cement previously described. The sealed tubes were then removed from the inert atmosphere box and the crystals examined more closely using a microscope. Crystals which appeared to be single were attached to a goniometer head and mounted to the Weissenberg camera. The goniometer head was manufactured by Charles Supper Company and contains two translational adjustments and two arc adjustments. The single crystal of $PrBr_3 \cdot 8DMSO$ was aligned in the Weissenberg camera so that a direct lattice axis could be rotated perpendicular to the x-ray beam. This allows a plane of atoms defined by two reciprocal axis to be rotated parallel to the x-ray beam. Weissenberg oscillation, rotation, and zero-level photographs were made before the crystal decomposed to the point that it could not be realigned. The reflections present on these photographs were used to determine the approximate reciprocal cell dimensions. Further attempts were made to obtain more and better Weissenberg photographs. The maximum number of patterns that could be produced before complete decomposition were one oscillation film, one rotation film, one zero-level film, and an incomplete first-layer film.

The oscillation photograph, Figure 16, showed the presence of m_x symmetry only. The m_x symmetry was evident because there was a reflection line coincident with the zero-layer line. The presence of m_x symmetry means that the crystal must belong to the monoclinic class or higher. If the class is monoclinic, the rotation axis must be the monoclinic unique axis, b (97).

Regardless of the crystal system, one of the direct lattice dimensions can be determined from the rotation photograph, Figure 17. The repeat distance, r, along the rotation axis can be calculated by Equa-

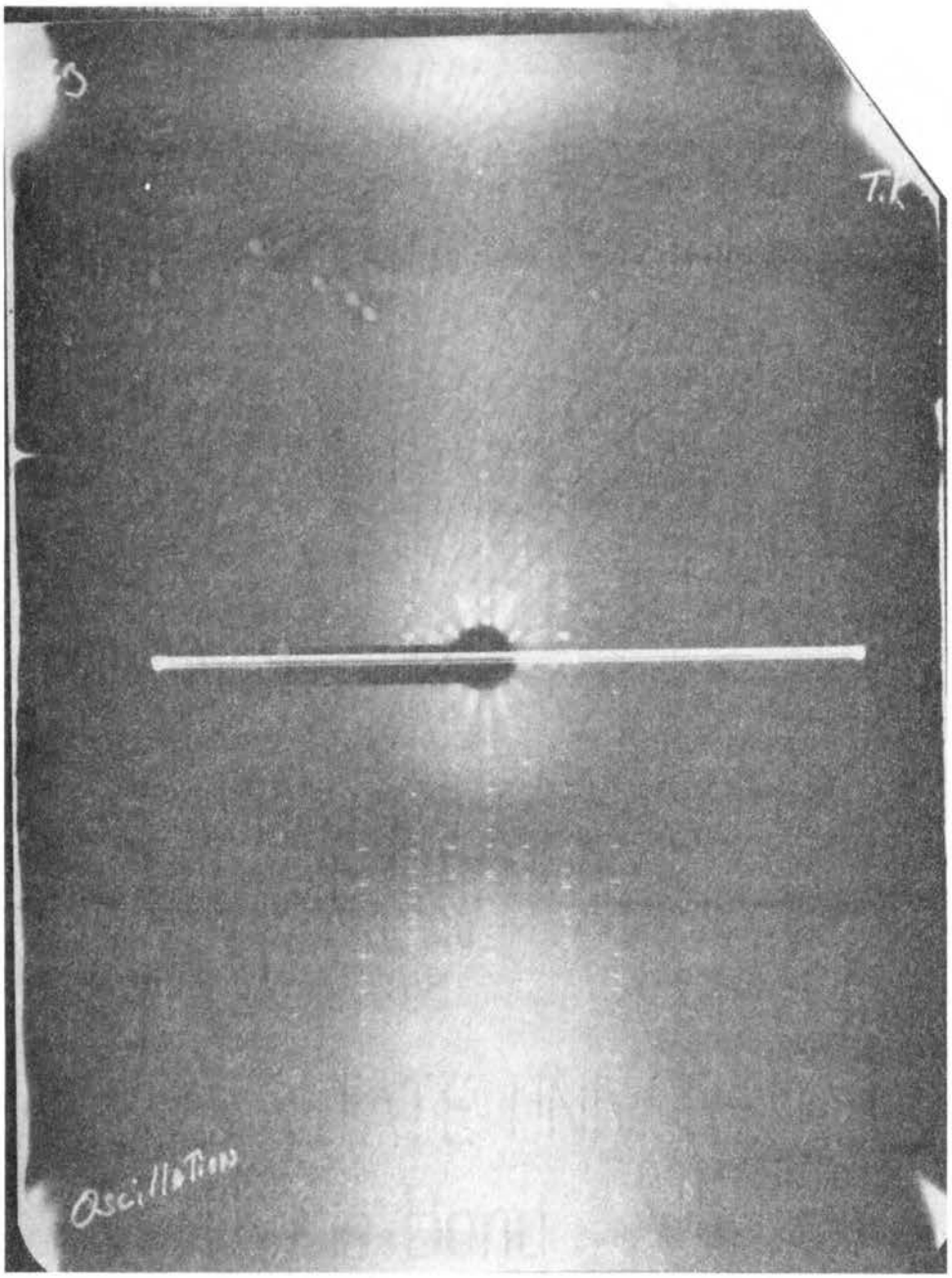

Figure 16. Weissenberg Oscillation Photograph of $PrBr_3 \cdot 8DMSO$

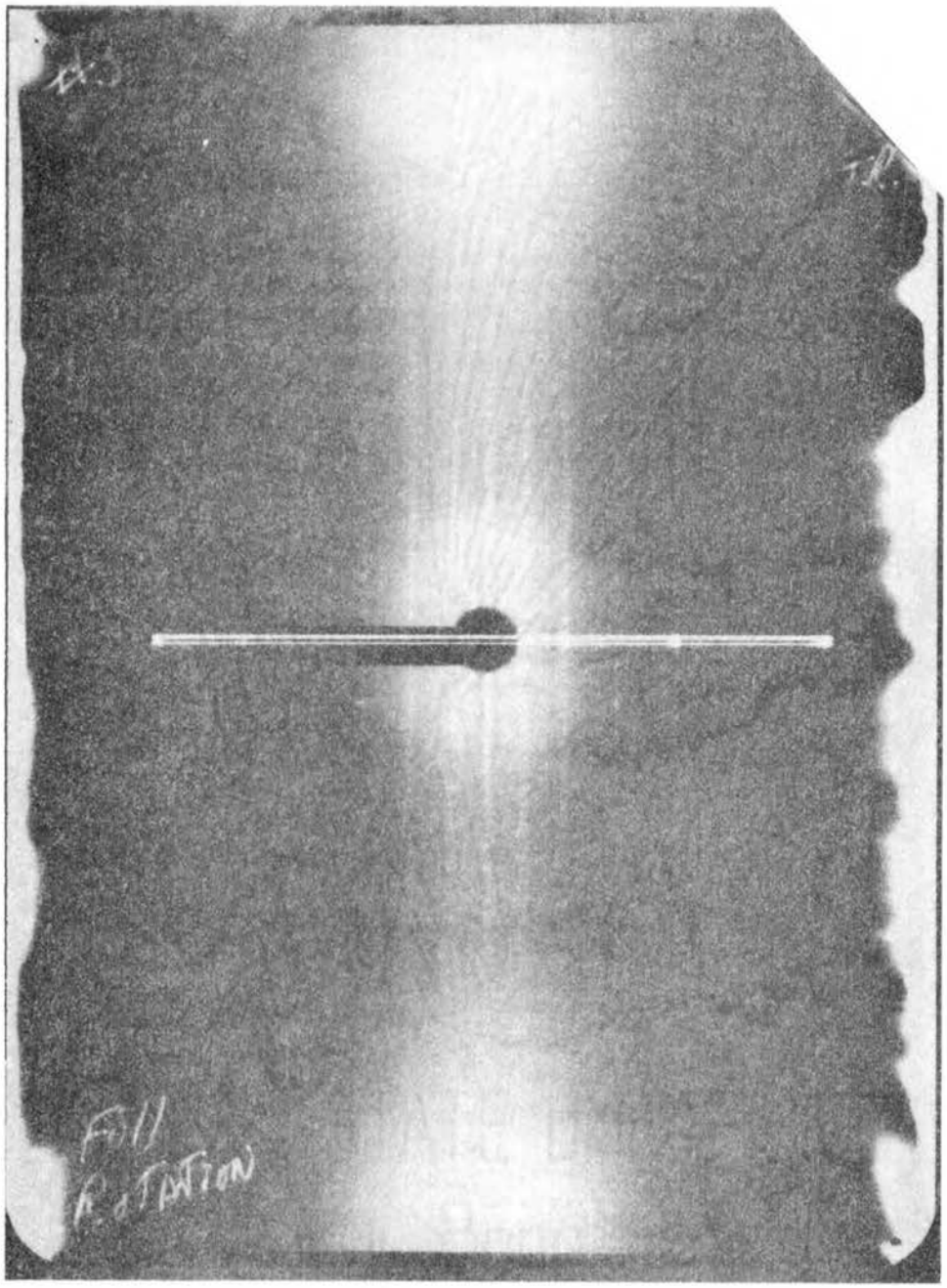

Figure 17. Weissenberg Rotation Photograph
$PrBr_3 \cdot 8DMSO$

tion 7 (97)

$$r = \frac{n\lambda}{\sin \tan^{-1}(y_n/R)} \qquad (7)$$

where n is the integral value for the layer line, λ is the wavelength of the x-rays, R is the radius of the camera, and y_n is the distance between the zero-layer line and the nth layer line is mm. For each layer line y_n was measured to the nearest 0.05 mm using the same device as was described for measuring the powder patterns. Calculated values of r are summarized in Table XIV. Values used that are not tabulated are: λ = 1.54178 Å and R = 28.65 mm. As indicated in Table XIV, the repeat distance along the rotation axis was approximately 9.07 Å. All other direct cell constants can be obtained from zero and upper-level Weissenberg photographs providing the crystal system can be identified.

TABLE XIV

CALCULATED VALUES OF DIRECT LATTICE LENGTH FROM WEISSENBERG ROTATION PHOTOGRAPH

n	y_n mm	y_n/R	$\sin \tan^{-1}(y_n/R)$	r Å
1	4.95	0.1728	0.170	9.07
2	10.40	0.3630	0.341	9.04
3	16.95	0.5916	0.509	9.09
4	26.50	0.9250	0.679	9.08
			Mean	9.07

The zero-level Weissenberg photograph of $PrBr_3 \cdot 8DMSO$ is shown in

Figure 18. Figure 19 is an extension of the zero-level using the same crystal oscillation. Absorption of the x-rays by the crystal was indicated by the light areas on the film. The zero-level photograph was indexed by means of Weissenberg templates purchased through Polycrystal Book Service. The shape of the festoons, curved lines connecting the diffraction spots, is determined by the geometry of the Weissenberg camera only. The only absent reflections were the odd integral values along one of the central lattice lines and the even integral values along the other central lattice line. The observed central lattice line reflections are circled in Figures 18 and 19. The broadening and splitting of the diffraction spots was due to the shape of the crystal (95) or the crystal decomposing and shifting to a misaligned position in the capillary tube. This broadening and splitting of the diffraction spots and extinctions due to absorption made it impossible to obtain precise film measurements. Upper-level Weissenberg photographs could not be obtained due to decomposition of the crystal. The m_x symmetry of the oscillation photograph indicated that the crystal was possibly monoclinic of point group m. However, upper-level Weissenberg photographs would be necessary to accurately determine the space group and crystal system. Monoclinic space groups, however, are relatively common for lanthanide complexes (25,43,46,51,62,63,93).

The dark line across the center of the zero-layer photograph, Figures 18 and 19, was the trace made by the undeflected x-ray beam as the film was translated parallel to the crystal axis of rotation. One of the angles in the reciprocal lattice was determined by measuring the distance between the two central lattice lines. The distance was measured from left to right parallel to the trace of the undeflected x-ray

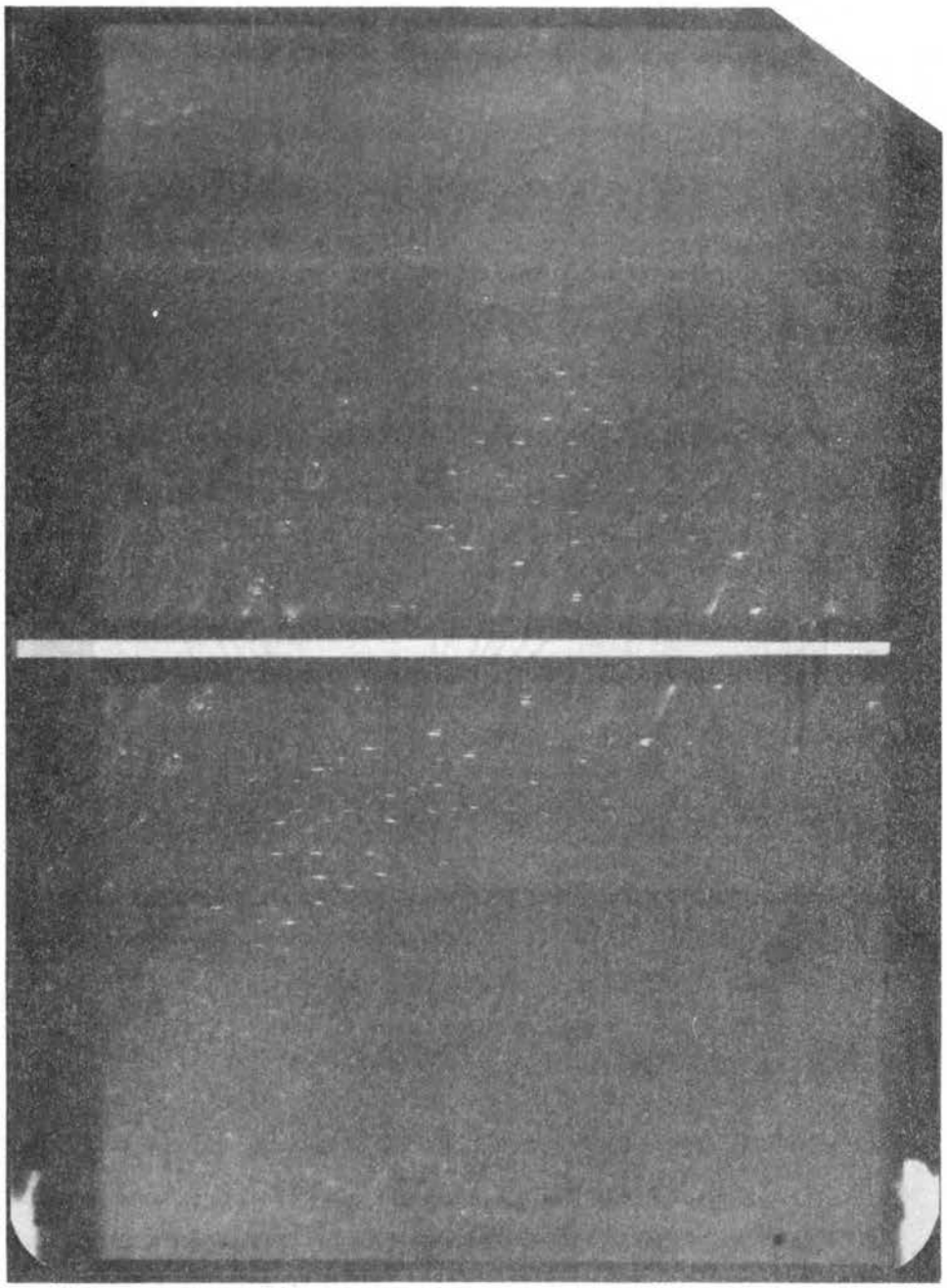

Figure 18. Weissenberg Zero-Level Photograph of $PrBr_3 \cdot 8DMSO$

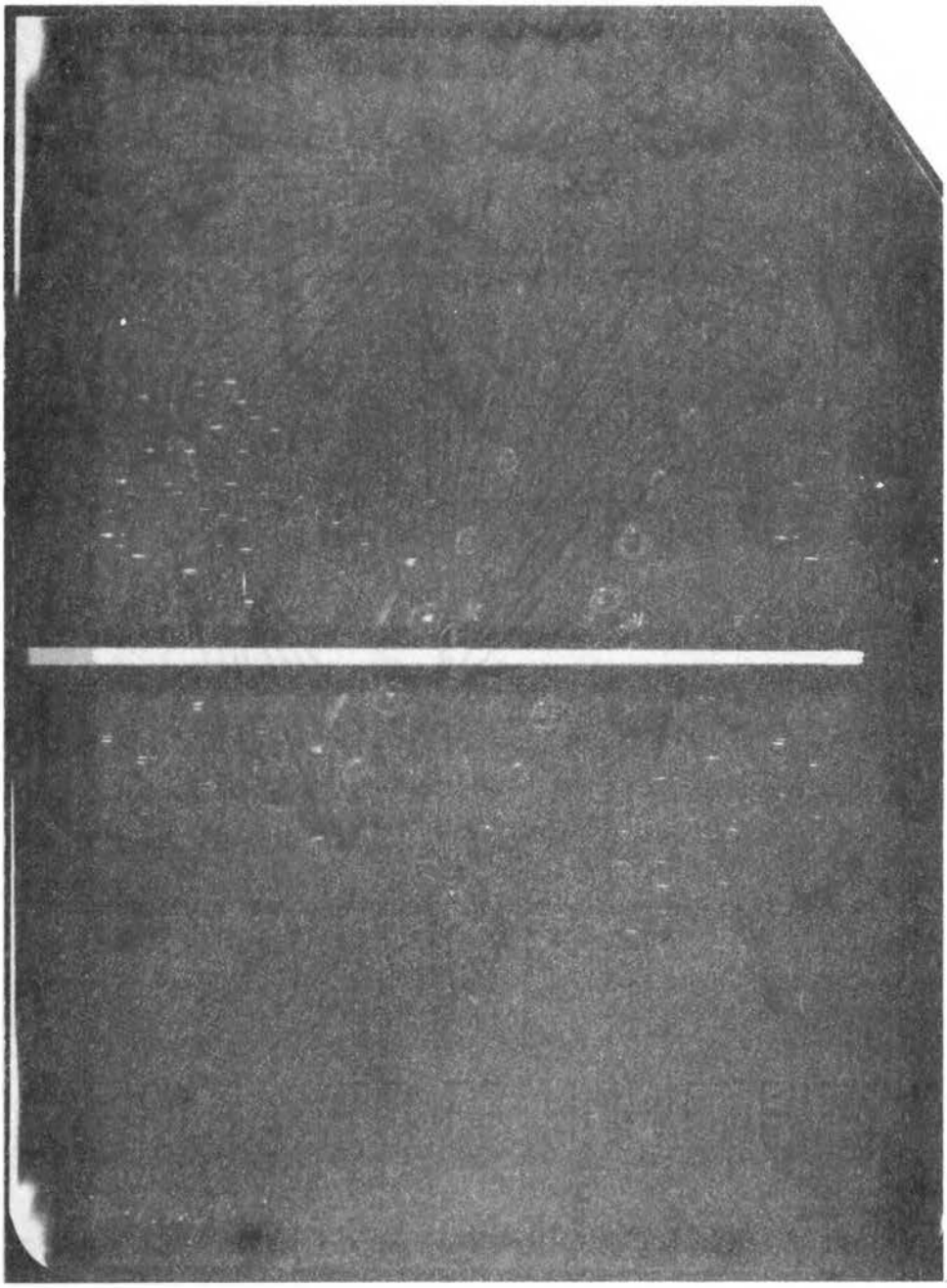

Figure 19. Translated Weissenberg Zero-Level Photograph of $PrBr_3 \cdot 8DMSO$

beam. The camera was designed so that 1 mm translation corresponds to 2° rotation of the crystal. The axis of rotation was assigned as being b* which was consistent with the observed symmetry of the oscillation photograph if a monoclinic crystal system was assumed. The distance between the central lattice lines was measured to determine the angle between the a* and b* axis, β^*. From Figure 18, a distance of 68.1 mm was measured which corresponds to an angle of 136.2°. From Figure 19, a distance of 21.9 mm was measured which corresponds to an angle of 43.8°. By convention, β^* is chosen to be the angle less than 90° and the assignment of the central lattice lines is made to correspond to a right hand coordinate system (97). By adding the central lattice line spacings in Figures 18 and 19, the repeat distance for any central lattice line was found to be 90 mm or 180°. This implies a negligible amount of film shrinkage and $\beta^* = 43.8^{\circ}$.

The axial repeat distance a* or c* was calculated from Equation 8 (97). In Equation 8, λ is the wavelength of the Cu K_{α} radiation, R is the radius

$$\text{axial repeat distance} = \frac{2}{n\lambda} \sin \left(\frac{2y(57.3)}{4R}\right) \tag{8}$$

of the camera, y is the perpendicular displacement in mm of a central lattice line point from the trace of the undeflected x-ray beam, and n is the index for the measured point. For a camera radius of 28.65 mm, Equation 8 is reduced to yield Equation 9.

$$\text{axial repeat distance} = \frac{2}{n\lambda} \sin y \tag{9}$$

The approximate values of a* and c* were found to be 0.0771 Å^{-1} and

0.0846 $\mathring{A}^{-1}$, respectively. Values for the axial repeat distance are the least accurately obtained values from Weissenberg photographs (97). Due to the preceeding and to difficulties with absorption and decomposition, the calculated values of a* and c* may differ greatly from the actual values.

Regardless of the crystal system, the volume of the direct unit cell, V, may be calculated by Equation 10 (97). The value of r was 9.07 $\mathring{A}$ as indicated in Table XIV.

$$V = \frac{1}{V^*} = \frac{r}{a^*c^*\sin \beta^*} \tag{10}$$

The volume of the unit cell was calculated to be approximately 2010 $\mathring{A}^3$. For Z = 2, the number of molecules per unit cell, the density, G, of the unit cell was calculated from Equation 11 (96). The calculated density of 1.662 g/cm^3 was in good agreement with the experimentally determined

$$G = \frac{Z(MW)(1.660 \times 10^{-24})}{V \times 10^{-24}} \tag{11}$$

density of 1.64 g/cm^3. The molecular weight, MW, of $PrBr_3 \cdot 8DMSO$ is 1005.756 as indicated by Table X. The experimental density was determined by the flotation method (97) which involved varying the proportions of a carbon tetrachloride/bromoform mixture until the crystals were just suspended in the mixture. The process was speeded up by the use of a Vortex test tube mixer and a centrifuge. When the crystals remained suspended after centrifuging, the density of the liquid and the density of the crystals were equal. Using the flotation method, the density of $PrBr_3 \cdot 8DMSO$ and $HoBr_3 \cdot 8DMSO$ were found to be 1.64 g/cm^3 and

1.83 g/cm^3, respectively. Assuming the two complexes are isomorphous as indicated by the powder patterns, the unit cell of the holmium complex has a volume of approximately 1880 Å^3. From the above, the dimensions of the unit cell of the holmium complex are about 0.98 of those of the praseodymium complex.

From Weissenberg photographs the reciprocal cell dimensions were determined to be: $a^* = 0.0771$ Å^{-1}, $b^* = 0.0846$ Å^{-1}, $\beta^* = 43.8^\circ$, and the distance between a*c* planes, r = 9.07 Å. Assuming the crystal was monoclinic, the unit cell dimensions were calculated from Equations 12 through 15 (97). Monoclinic unit cell dimensions were calculated to be:

$$a = \frac{1}{a^* \sin \beta^*} \tag{12}$$

$$b = \frac{1}{b^*} = r \tag{13}$$

$$c = \frac{1}{c^* \sin \beta^*} \tag{14}$$

$$\beta = 180^\circ - \beta^* \tag{15}$$

a = 18.7 Å, b = 9.07 Å, c = 17.1 Å, and $\beta = 136.2^\circ$. The unit cell dimensions were compared to the $\sin^2\theta$ values (Table XII) obtained from x-ray powder patterns by Equations 16 through 19 (94). The calculated values of $\sin^2\theta$ compared approximately with the values of $\sin^2\theta$ listed in Table XII, and agreement was as good as could be expected due to the problems encountered for both the powder and Weissenberg measurements.

$$\sin^2\theta_{hk\ell} = h^2A + \ell^2C + 2h\ell\sqrt{AC}\cos\beta + k^2B \tag{16}$$

$$A = \frac{\lambda^2}{4a^2\sin^2\beta} \tag{17}$$

$$B = \frac{\lambda^2}{4b^2} \tag{18}$$

$$C = \frac{\lambda^2}{4c^2 \sin^2 \beta} \tag{19}$$

Conclusions From X-Ray Data

Neither the powder photographs nor the Weissenberg photographs produced very precise results. The major factors limiting the precision of the results were the absorption of x-rays by the sample and decomposition of the complexes in the x-ray beam. The x-ray study, however, was very important in that the powder patterns indicated that crystals of $PrBr_3 \cdot 8DMSO$ and $HoBr_3 \cdot 8DMSO$ were very similar with slightly smaller lattice dimensions for the holmium complex. The Weissenberg photographs verified that the complexes could be produced as single crystals. Approximate lattice dimensions were calculated from the Weissenberg photographs. The density of the unit cell calculated from dimensions obtained from the Weissenberg photographs was in good agreement with the experimentally determined density. If better Weissenberg photographs could have been obtained, the structure of the complexes and the precise coordination of the lanthanide ions could be determined.

CHAPTER V

SUMMARY AND SUGGESTIONS FOR FUTURE STUDY

Many coordination compounds of the lanthanides have been prepared and their coordination numbers assigned, as shown in Table II. In this study, a coordination number of eight was determined for both praseodymium and holmium complexes with DMSO. A reported coordination number of eight for the lanthanides is fairly common; however, most researchers have assigned different coordination numbers for praseodymium and holmium (Table II).

It was found that techniques reported in the literature for preparing lanthanide complexes with DMSO frequently produced a finely divided solid. Examination of the solid indicated the presence of glasses or of crystalline particles suspended in a glass. Published analytical results (30,34,45,52) for DMSO complexes of the lanthanides consistently show a higher than ideal percentage composition of DMSO. In this study, crystals of $PrBr_3 \cdot 8DMSO$ and $HoBr_3 \cdot 8DMSO$ with well defined faces were chosen. The analytical results, Chapter II, showed only a slight deviation from the ideal value for stoichiometric composition of DMSO. Before detailed analytical studies of solid complexes are conducted, it is suggested that the nature of the solid first be established. This study has shown that more precise analytical results can be obtained when well defined crystals are grown.

Molecular weight measurements of $PrBr_3 \cdot 8DMSO$ and $HoBr_3 \cdot 8DMSO$ in

acetonitrile indicated that both complexes dissociate to produce 3.9 particles per mole of complex. This type of behavior has also been reported for conductance measurements for other lanthanide-halide complexes. This behavior was taken as indicative of outer sphere coordination of lanthanide ions by halide ions.

The vibrational spectra of the complexes were recorded using both laser Raman and infrared methods, Chapter III. The Raman and infrared active bands were recorded for both coordinated and uncoordinated DMSO. When DMSO was coordinated with praseodymium or holmium, the frequency of the DMSO vibrational modes were observed to usually shift to higher frequencies than those observed for the uncoordinated DMSO. Both $PrBr_3 \cdot 8DMSO$ and $HoBr_3 \cdot 8DMSO$ showed no frequencies that could be assigned to uncoordinated DMSO. This indicated that all eight of the ligand molecules in each complex were equivalent. The relative shift of the DMSO bands indicated that the DMSO molecules were more strongly bound in the holmium complex than in the praseodymium complex. Both complexes showed a decrease in the frequency of the S=O stretching mode. This shift indicated coordination through the oxygen atom of the DMSO molecule. A low frequency band in the range of 80 to 90 cm^{-1} was observed for both complexes and was assigned to a M-O mode.

Assuming that the bromide ions were not in the primary coordination sphere, a coordination number of eight was established for both praseodymium and holmium. The coordination of lanthanide ions is predominately determined by charge density values. The steric hinderances imposed by the smaller ionic radius of holmium was more than compensated for by the increase in charge density and praseodymium and holmium have the same coordination number in DMSO complexes.

The holmium complex was found to have a smaller unit cell volume than the praseodymium complex. This was observed by density determinations and also by the d spacings of the x-ray powder diffraction patterns. Even though there was a decrease in the unit cell volume, the two complexes were found to be very similar.

Weissenberg x-ray photographs were taken to verify that the complexes could be produced as single crystals. Based on the symmetry of the unit cell as determined from the Weissenberg photographs, the crystals apparently belong to the monoclinic crystal system. Approximate values for the reciprocal cell constants were calculated for $PrBr_3 \cdot 8DMSO$. The crystal was found to contain two molecules of the complex per unit cell. Cu K_α radiation, $\lambda = 1.54178$ Å, and x-ray film were used to record all of the diffraction patterns. The recorded patterns were of relatively poor quality mainly due to the tendency of the complexes to decompose and to absorb the Cu K_α radiation.

The best way to study the coordination of the lanthanides would be to determine the structures of all of the lanthanide ions with the same ligands. The only method of determining precise molecular structure is by single crystal x-ray diffraction. The rate of decomposition of lanthanide complexes could perhaps be reduced by recording the diffraction patterns at very low temperatures. Absorption problems could be reduced by using x-rays of a shorter wavelength such as Mo K_α, $\lambda = 0.7107$ Å. Due to the poor response of x-ray film to Mo K_α radiation, the best results would be obtained by using a counting diffractometer. A structure determination for the complexes in this study would yield the metal-bromide and the metal-oxygen distances. The coordination number could then be determined without making assumptions regarding the coordination in the solid versus the coordination in solution.

A SELECTED BIBLIOGRAPHY

(1) Cotton, A. F. and G. Wilkinson, Advanced Inorganic Chemistry, Interscience Publishers, 1962, pp. 870.

(2) Spedding, F. H. and A. H. Daane, eds., The Rare Earths, John Wiley and Sons, Inc., New York and London, 1961, pp. 4.

(3) Moeller, T., The Chemistry of the Lanthanides, Reinhold Publishing Corporation, New York, 1963, pp. 7.

(4) Oguar, N. and T. Nanya, Nature, 212, 757 (1966).

(5) Larsson, R., Record of Chem. Prog., 31, 171 (1970).

(6) Darensbourg, M. Y. and D. J. Darensbourg, J. Chem. Educ., 47, 33 (1970).

(7) Weber, J. H., Inorg. Nucl. Chem. Lett., 5, 737 (1969).

(8) Berney, C. V. and J. H. Weber, Inorg. Chem., 7, 283 (1968).

(9) Selbin, J., W. E. Bull, and L. H. Holmes, Jr., J. Inorg. Nucl. Chem., 16, 219 (1961).

(10) Holser, W. T., J. Chem. Educ., 36, 79 (1959).

(11) Cotton, F. A., R. Francis, and W. D. Horrocks, Jr., J. Phys. Chem., 64, 1534 (1960).

(12) Meek, D. W., D. K. Straub, and R. S. Drago, J. Amer. Chem. Soc., 82, 6013 (1960).

(13) Moeller, T., J. Chem. Educ., 47, 417 (1970).

(14) Zachariasen, W. H., in Seaborg, G. T. and J. J. Katz, eds., The Actinide Elements, McGraw-Hill Book Co., New York, Chap. 18 (1954).

(15) Gschneidner, K. A., Jr., J. Less-Common Metals, 25, 405 (1971).

(16) Dzhurinskii, B. F. and G. A. Pandurkin, Seminar Spektrosk. Svoistvam Lyuminoforov, Aktiv. Redk. Zemlyami, 2nd 1969, 70. From Ref. Zh. Khim. 1971, Abstr. No. 12B26, via C. A., 77, 118422g (1972).

(17) Johnson, O., J. Chem. Educ., 47, 431 (1970).

(18) Katzin, L. I. and M. L. Barnett, J. Phys. Chem., 68, 3779 (1964).

(19) Volkov, V. M., et al., Zh. Strukt. Khim., 11, 331 (306 Eng.) (1970).

(20) Siekierski, S., J. Inorg. Nucl. Chem., 32, 519 (1970).

(21) Domrachev, G. A., M. I. Gryaznova, V. P. Ippolitova, Seminar Spektrosk. Svoistvam Lyuminoforov, Aktiv. Redk. Zemlyami, 2nd 1969, 81. From Ref. Zh. Zhim. 1971, Abstr. No. 11B187, via C. A., 77, 11949g (1972).

(22) Spacu, P. and S. Plostinaru, Rev. Roum. Chim., 18, 971 (1973).

(23) Karraker, D. G., J. Chem. Educ., 47, 424 (1970).

(24) Charpentier, L. J. and T. Moeller, J. Inorg. Nucl. Chem., 32, 3575 (1970).

(25) Bhandary, K. K. and H. Manohar, Acta Crystallogr., 29B, 1093 (1973).

(26) Sinha, S. P., Complexes of the Rare Earths, Permagon Press, 1966, p. 17.

(27) Moeller, T., R. L. Dieck, and J. E. McDonald, Rev. Chim. Miner., 10, 177 (1973).

(28) Miller, W. V. and S. K. Madan, J. Inorg. Nucl. Chem., 30, 2785 (1968).

(29) Zinner, L. B. and G. Vicentini, Inorg. Nucl. Chem. Lett., 7, 967 (1971).

(30) Iwase, A. and S. Tada, Nippon Kagaku Kaishi, No. 1, 60 (1973).

(31) Spacu, P. and E. Ivan, Rev. Roum. Chim., 18, 589 (1973).

(32) Forsberg, J. H. and T. Moeller, Inorg. Chem., 8, 883 (1969).

(33) Kutek, F., Collect. Czech. Chem. Commun., 33, 1341 (1968), via C. A., 68, 110918s (1968).

(34) Ramalingam, S. K. and S. Soundararajan, Inorg. Nucl. Chem., 29, 1763 (1967).

(35) Cannon, J. C., Ph.D. Thesis, Oklahoma State University, Stillwater, Okla., 1973.

(36) Muetterties, E. L. and C. M. Wright, Quart. Rev. (London), 21, 109 (1967).

(37) Horrocks, W. D., Jr., J. P. Sipe, III, and J. R. Luber, J. Amer. Chem. Soc., 93, 5258 (1971).

(38) Birnbaum, E. R. and S. Stratton, Inorg. Chem. 12, 379 (1973).

(39) Muetterties, E. L., Inorg. Chem., 4, 769 (1965).

(40) Hoard, J. L. and J. V. Silverton, Inorg. Chem., 2, 235 (1963).

(41) Powell, J. E. and D. L. G. Rowlands, Inorg. Chem., 5, 819 (1966).

(42) Coda, A., G. Giuseppetti, and C. Tadini, Periodico Mineral., 34, 27 (1965), via C. A., 63, 12434g (1965).

(43) Lind, M. D., B. Lee and J. L. Hoard, J. Amer. Chem. Soc., 94, 1611 (1965).

(44) Al-Karaghouli, A. R. and J. S. Wood, Inorg. Chem., 11, 2293 (1972).

(45) Krishnamurthy, V. N. and S. Soundararajan, J. Inorg. Nucl. Chem., 29, 517 (1967).

(46) Bhandary, K. K. and H. Manohar, Indian J. Chem., 9, 275 (1971).

(47) Giesbrecht, E. and M. Kawashita, J. Inorg. Nucl. Chem., 32, 2461 (1970).

(48) Oskarsson, A., Acta. Chem. Scand., 25, 1206 (1971).

(49) Brecher, C., A. Lempicki, and H. Samelson, J. Chem. Phys., 41, 279 (1964).

(50) Zalkin, A., D. H. Templeton, and D. G. Karraker, Inorg. Chem., 8, 2680 (1969).

(51) Korytnyi, E. F., et al., Zh. Strukt. Khim., 11, 311 (289 Eng.) (1970).

(52) Ramalingam, S. K. and S. Soundararajan, Z. Anorg. Allg. Chem. 353, 216 (1967).

(53) Cramer, R. E. and K. Seff, J. Chem. Soc., Chem. Commun., 400 (1972).

(54) Erasmus, C. S. and J. C. A. Boeyens, Acta Crystallogr., 26B, 1843 (1970).

(55) Thompson, L. C., J. Inorg. Nucl. Chem., 24, 1083 (1962).

(56) Ramalingam, S. K., and S. Soundararajan, Curr. Sci., 35, 568 (1966).

(57) Ramalingam, S. K. and S. Soundararajan, Bull. Chem. Soc. Jap., 41, 106 (1968).

(58) Przystal, J. K., W. G. Bos, and I. B. Liss, J. Inorg. Nucl. Chem., 33, 679 (1971).

(59) Katyal, M., et al., Curr. Sci., 35, 389 (1966).

(60) Ramalingam, S. K. and S. Soundararajan, Curr. Sci., 35, 233 (1966).

(61) Manning, P. G., Can. J. Chem., 41, 2557 (1963).

(62) Uebel, J. J. and R. M. Wing, J. Amer. Chem. Soc., 94, 8910 (1972).

(63) Cramer, R. E. and K. Seff, Acta Crystallogr., B28, 3281 (1972).

(64) Stewart, W. E. and T. H. Siddall, III., J. Inorg. Nucl. Chem., 32, 3599 (1970).

(65) Arthur, P., W. M. Haynes, and L. P. Varga, Anal. Chem., 38, 1630 (1966).

(66) Eubanks, I. D. and F. J. Abbott, Anal. Chem., 41, 1708 (1969).

(67) Lyle, S. J. and M. Rahman, Talanta, 10, 1177 (1963).

(68) Skoog, D. A., and D. M. West, Analytical Chemistry, Holt, Rinehart and Winston, 1965.

(69) Douglas, T. B., J. Am. Chem. Soc., 68, 1072 (1946).

(70) Traynelis, V. J. and W. L. Hergenrother, J. Org. Chem., 29, 221 (1964).

(71) McNew, R. W., Oklahoma State University, personal communication, 1973.

(72) Snedecor, G. W. and W. G. Cochran, Statistical Methods, The Iowa State University Press, 1967, Chapter 9.

(73) Yatsimirskii, K. B., et al., Teor. i Eksperim. Khim., Akad. Nauk Ukr. SSR 1(1), 100 (1965), via C. A., 63, 3769e (1965).

(74) Choppin, G. R. and S. L. Bertha, J. Inorg. Nucl. Chem., 35, 1309 (1973).

(75) Operation Manual, Hitachi-Perkin-Elmer Model 115 Molecular Weight Apparatus, Perkin-Elmer Co.

(76) Albescu, I., Rev. Roum. Chim., 18, 599 (1973).

(77) Prado, J. C. and G. Vicentini, Inorg. Nucl. Chem. Lett., 9, 693 (1973).

(78) Dutt, N. K. and D. Majumdar, J. Inorg. Nucl. Chem., 34, 657 (1972).

(79) Bulkin, B. J., J. Chem. Educ., 46, A859 (1969).

(80) Sloane, H. J., Applied Spec. 25, 430 (1971).

(81) Bulkin, B. J., J. Chem. Educ. 46, A781 (1969).

(82) Evans, J. C., Advan. Anal. Chem. Instrum., 7, 41 (1968).

(83) Tobias, R. S., J. Chem. Educ., 44, 2 (1967).

(84) Kettle, S. F. A., Coordination Compounds, Universities Press, Belfast, 1969, p. 151.

(85) Martell, A. E., Coordination Chemistry, Volume 1, Van Nostrand Reinhold Company, New York, 1971, p. 149.

(86) Currier, W. F. and J. H. Weber, Inorg. Chem., 6, 1539 (1967).

(87) Smith, D. E., Ph.D. Thesis, Oklahoma State University, Stillwater, Okla., 1971.

(88) Drig, J. R., C. M. Player, and J. Bragin, J. Chem. Phys., 52, 4224 (1970).

(89) Ramaswamy, K. and S. Swaminathan, Indian J. Pure Appl. Phys., 7, 807 (1969).

(90) Horrocks, W. D., Jr. and F. A. Cotton, Spectrochim. Acta, 17, 134 (1961).

(91) Ramaswamy, K. and S. Swaminathan, Indian J. Pure. Appl. Phys., 7, 671 (1969).

(92) Salonen, A. K., Ann. Acad. Sci. Fennicae Ser., A6(67), 1(1961), via C. A., 55, 20624a (1961).

(93) Einstein, F. W. B. and D. G. Tuck, J. Chem. Soc., Chem. Commun., 1182 (1970).

(94) Azaroff, L. V. and M. J. Buerger, The powder method, McGraw-Hill Book Company, New York, 1958.

(95) Buerger, M. J., X-Ray Crystallography, John Wiley & Sons, Inc., New York, 1942.

(96) Buerger, M. J., Crystal-structure analysis, John Wiley & Sons, Inc., New York, 1960.

(97) Stout, G. H. and L. H. Jensen, X-Ray Structure Determination, The MacMillan Company, London, 1968.

(98) Woolfson, M. M., X-Ray Crystallography, Cambridge at the University Press, 1970.

(99) Nuffield, E. W., X-Ray Diffraction Methods, John Wiley & Sons, Inc., New York, 1966.

(100) Baun, W. L., Air Force Systems Command, RTD-TDR-63-4202, 3 (1963).

(101) Zachariasen, W. H., U. S. Atomic Energy Comm., TID-5212, 157 (1955).

VITA

Charles Lee Riggs

Candidate for the Degree of

Doctor of Philosophy

Thesis: SYNTHESIS AND CHARACTERIZATION OF CRYSTALLINE COMPLEXES OF DIMETHYL SULFOXIDE WITH HOLMIUM AND PRASEODYMIUM BROMIDES

Major Field: Chemistry

Biographical:

Personal Data: Born in Clayton, New Mexico, August 21, 1946, the son of Mr. and Mrs. Everett E. Riggs.

Education: Graduated from Weatherford High School, Weatherford, Oklahoma, in May, 1964; received the Bachelor of Science degree from Southwestern State College, Weatherford, Oklahoma, with a double major in Mathematics and Chemistry in May, 1967; and completed the requirements for the Doctor of Philosophy degree at Oklahoma State University in May, 1974.

Professional Experience: Stockroom Manager, Department of Chemistry, Southwestern State College from 1965 to 1967; graduate teaching assistant, Chemistry Department, Oklahoma State University, from 1967 to 1968 and from 1970 to 1973; X-Ray Technician, Continental Oil Company, Summer 1968.

Professional Organizations: American Chemical Society, Phi Lambda Upsilon honorary chemical society, American Association for the Advancement of Science.